

AD-A182 525

NEW CONCEPT FOR SCALING EXCIMER LASER AMPLIFIERS(U)
SCIENCE RESEARCH LAB INC SOMERVILLE MA R WATTERSON
30 JUN 87 SRL-84-F-1987 N00014-85-C-8740

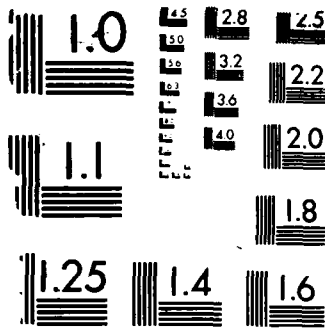
1/1

UNCLASSIFIED

F/G 20/5

NL

												
									END 8-81 DTU			



MICROCOPY RESOLUTION TEST CHART

U.S. GOVERNMENT PRINTING OFFICE: 1963 O 344-100

12

DTIC FILE COPY

REPORT SRL-04-F-1987

NEW CONCEPT FOR SCALING EXCIMER LASER AMPLIFIERS

Prepared by
Dr. Reich Watterson

SCIENCE RESEARCH LABORATORY, INC.
15 Ward Street
Somerville, MA 02143

30 June 1987

FINAL TECHNICAL REPORT
Period for October 1, 1985 to April 30, 1987
Contract Number N00014-85-C-0740

AD-A182 525

APPROVED FOR PUBLIC RELEASE; DISTRIBUTION UNLIMITED

Prepared for
OFFICE OF NAVAL RESEARCH
800 North Quincy Street
Arlington, VA 22217-5000

DTIC
FILE COPY
JUL 06 1987
S A

"The views and conclusions contained in this document are those of the authors and should not be interpreted as representing the official policies, either expressed or implied, of the Strategic Defense Initiative Organization or the U.S. Government."

REPORT DOCUMENTATION PAGE

Form Approved
OMB No. 0704-0188
Exp. Date: Jun 30, 1986

1a. REPORT SECURITY CLASSIFICATION Unclassified		1b. RESTRICTIVE MARKINGS None	
2a. SECURITY CLASSIFICATION AUTHORITY N/A		3. DISTRIBUTION/AVAILABILITY OF REPORT Unlimited	
2b. DECLASSIFICATION/DOWNGRADING SCHEDULE N/A			
4. PERFORMING ORGANIZATION REPORT NUMBER(S) 04/F/1987		5. MONITORING ORGANIZATION REPORT NUMBER(S)	
6a. NAME OF PERFORMING ORGANIZATION Science Research Laboratory	6b. OFFICE SYMBOL (if applicable)	7a. NAME OF MONITORING ORGANIZATION Office of Naval Research	
6c. ADDRESS (City, State, and ZIP Code) 15 Ward St. Somerville, MA 02143		7b. ADDRESS (City, State, and ZIP Code) Dept. of the Navy 800 N. Quincy St. Arlington, VA 22217-5000	
8a. NAME OF FUNDING/SPONSORING ORGANIZATION SDIO	8b. OFFICE SYMBOL (if applicable)	9. PROCUREMENT INSTRUMENT IDENTIFICATION NUMBER N00014-85-C-0740	
8c. ADDRESS (City, State, and ZIP Code) Pentagon Washington, DC		10. SOURCE OF FUNDING NUMBERS	
		PROGRAM ELEMENT NO.	PROJECT NO. NRSDW208/ 8-2-85(111210)
		TASK NO.	WORK UNIT ACCESSION NO.
11. TITLE (Include Security Classification) New Concept for Scaling Excimer Laser Amplifiers			
12. PERSONAL AUTHOR(S) Reich Watterson			
13a. TYPE OF REPORT Final Technical	13b. TIME COVERED FROM 10/1/85 TO 4/30/87	14. DATE OF REPORT (Year, Month, Day) 87/6/30	15. PAGE COUNT
16. SUPPLEMENTARY NOTATION			
17. COSATI CODES		18. SUBJECT TERMS (Continue on reverse if necessary and identify by block number)	
FIELD	GROUP	SUB-GROUP	
19. ABSTRACT (Continue on reverse if necessary and identify by block number)			
<p>A novel concept for efficient volumetric scaling of excimer lasers to high average power and energy was theoretically and experimentally investigated. Numerical calculations of the extraction efficiency of an excimer laser amplifier with a nonsaturable distributed loss are described. These results show that expanding the beam as it traverses the amplifier can lead to considerably improved extraction efficiency. Expansion angles of 2 to 5 degrees are useful for large scale laser amplifiers (10 meters in length).</p> <p>A small scale proof-of-principle experiment was constructed. This consisted of an electron beam pumped XeCl master oscillator-amplifier system. A 250 kV electron beam pumped a 11 cm x 11 cm x 100 cm active volume which served as both a oscillator and as an amplifier.</p> <p>Measurements of the extraction efficiency were performed for collimated,</p>			
20. DISTRIBUTION/AVAILABILITY OF ABSTRACT <input checked="" type="checkbox"/> UNCLASSIFIED/UNLIMITED <input type="checkbox"/> SAME AS RPT <input type="checkbox"/> DTIC USERS		21. ABSTRACT SECURITY CLASSIFICATION Unclassified	
22a. NAME OF RESPONSIBLE INDIVIDUAL Jonah Jacob		22b. TELEPHONE (Include Area Code) 617-547-1122	22c. OFFICE SYMBOL

UNCLASSIFIED

19. ABSTRACT CONTINUED

cylindrically expanding, and spherically expanding beams. An expansion angle of approximately 0.6 degrees led to an improvement of as much as a factor of 2 in integrated extraction efficiency.

Accession For	
NTIS SPARI	<input checked="" type="checkbox"/>
DTIC TAB	<input type="checkbox"/>
Unannounced	<input type="checkbox"/>
Justification	
By	
Distribution/	
Availability Codes	
List	Avail. and/or Special
+	✓



SUMMARY

A novel concept for efficient volumetric scaling of excimer lasers to high average power and energy was theoretically and experimentally investigated. Numerical calculations of the extraction efficiency of an excimer laser amplifier with a nonsaturable distributed loss are described. These results show that expanding the beam as it traverses the amplifier can lead to considerably improved extraction efficiency. Expansion angles of 2 to 5 degrees are useful for large scale laser amplifiers (10 meters in length).

A small scale proof-of-principle experiment was constructed. This consisted of an electron beam pumped XeCl master oscillator-amplifier system. A 250 kV electron beam pumped a 11 cm \times 11 cm \times 100 cm active volume which served as both a oscillator and as an amplifier.

Measurements of the extraction efficiency were performed for collimated, cylindrically expanding, and spherically expanding beams. An expansion angle of ~ 0.6 degrees led to an improvement of as much as a factor of 2 in integrated extraction efficiency.

TABLE OF CONTENTS

<u>Chapter</u>	<u>Page</u>
List of Illustrations	v
1 INTRODUCTION	1-1
2 PERFORMANCE OF EXPANDING WAVE LASER AMPLIFIERS	2-1
2.1 Introduction	2-1
2.2 Comparative Analysis of Expanding Wave Amplifiers and Conventional Amplifiers	2-1
3 PROOF OF PRINCIPLE EXPERIMENT	3-1
3.1 Introduction	3-1
3.2 Pulsed Power and Magnetic Field Design	3-1
3.3 Laser Oscillator Resonator Design	3-9
4 EXPERIMENTAL RESULTS	4-1
4.1 Introduction	4-1
4.2 Laser Diagnostics	4-1
4.3 Extraction Measurements	4-3
REFERENCES	5-1

Document

- A Expanding Beam Concept for Building Very Large Excimer Laser Amplifiers 6-1

LIST OF ILLUSTRATIONS

<u>Figure</u>		<u>Page</u>
1.1	Conventional Electron Beam Pumped Laser Geometry	1-2
1.2	Expanding Wave Laser Amplifier Geometry	1-3
2.1	Extraction Efficiency as a Function of Amplifier Length for a Conventional Rectangular Amplifier and $\phi_{in} = 0.1$	2-3
2.2	Extraction Efficiency as a Function of Amplifier Length for a Conventional Rectangular Amplifier and $\phi_{in} = 1.0$	2-4
2.3	Schematic Geometry of an Expanding Wave Laser Amplifier	2-6
2.4	Comparison of Integrated Extraction Efficiency for Collimated and Expanding Beams for $\phi_{in} = 0.1$	2-7
2.5	Comparison of Integrated Extraction Efficiency for Collimated and Expanding Beams for $\phi_{in} = 1.0$	2-8
2.6	Comparison of Integrated Extraction Efficiency for Collimated and Expanding Beams for $\phi_{in} = 1.5$	2-9
2.7	Extraction Efficiency at Fixed Amplifier Length for Collimated, Cylindrical and Spherical Expansion	2-11
3.1	Laser Cross Section Showing Electron Beam Pumped Master Oscillator-Amplifier Configuration	3-2
3.2	Block Diagram of Expanding Beam Laser Amplifier Proof of Principle Experiment	3-3
3.3	Electron Beam Current and Voltage	3-6
3.4	High Voltage Termination Equipotentials in Highest Electric Stress Region	3-7
3.5	Photograph of Assembled Cable and Termination Assembly	3-8

3.6	Photograph of Assembled Laser System Showing Magnets and Cable Pulsed Power Supply	3-12
4.1	Optical Layout of the Expanding Beam Laser Amplifier Experiment	4-2
4.2	Typical XeCl Laser Shot	4-4
4.3	Measured Extraction Efficiency for a Collimated Beam as a Function of Input Flux Density	4-5
4.4	Measured Extraction Efficiency of a Cylindrically Expanding Beam Compared to a Collimated Beam	4-6
4.5	Measured Extraction Efficiency of a Spherically Expanding Beam Compared to a Collimated Beam	4-7
4.6	Photodiode Records of Laser and Amplified Outputs: (a) Amplified Collimated and (b) Injected Beams	4-8
4.7	Photodiode Records of Laser and Amplified Outputs: (a) Amplified Expanding and (b) Injected Beams	4-9

CHAPTER 1

INTRODUCTION

The experimental verification of a novel concept for efficient volumetric scaling of excimer lasers to high average power and energy is reported here. This concept will permit efficient scaling of excimer lasers to energy and power levels a factor of ten larger than allowed by conventional approaches.

The conventional architecture for building an electron beam pumped excimer laser is shown in Fig. 1.1. The active medium, rectilinear in shape, is pumped by two high energy electron beams that penetrate the high pressure laser mixture from two opposing faces of the laser cavity. The laser gas flows in a direction normal to the electron beam propagation. The optical beam is extracted in the direction orthogonal to both the electron beam and flow directions. For an active medium which has a nonsaturable absorption, the efficiency of energy extraction possible from a laser of this geometry decreases precipitously for absorption length products exceeding unity. In such long amplifiers the optical flux is amplified along the length to such a level that the gain decreases due to saturation. The non saturable absorption loss, however, remains unchanged thus decreasing the efficiency of extracting photons from the active medium.

The expanding wave laser concept reported here removes this constraint by more closely maintaining the optimum cavity flux density for energy extraction by expanding the optical beam as shown in Fig. 1.2. Such an expansion can be accomplished by injecting spherically or cylindrically expanding beams into the amplifier. In Chapter 2 the amplifier equation is solved numerically and is used to show that this concept can result in an efficiency improvement of a factor of two over the conventional rectilinear geometry in large scale amplifiers. It is also shown that the angle at which the laser beam must be expanded is relatively small, 2 to 5 degrees. These small expansions allow the use of flow

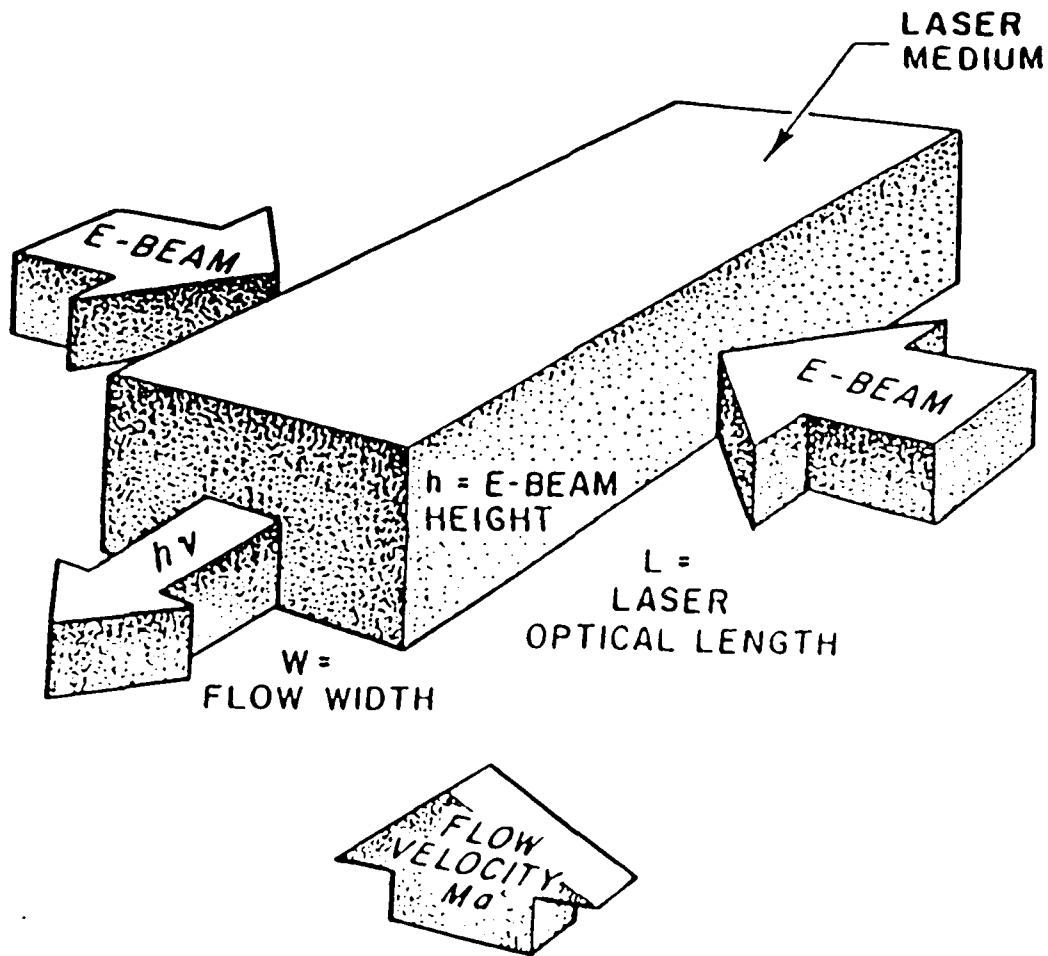


Figure 1.1: Conventional Electron Beam Pumped Excimer Laser Geometry

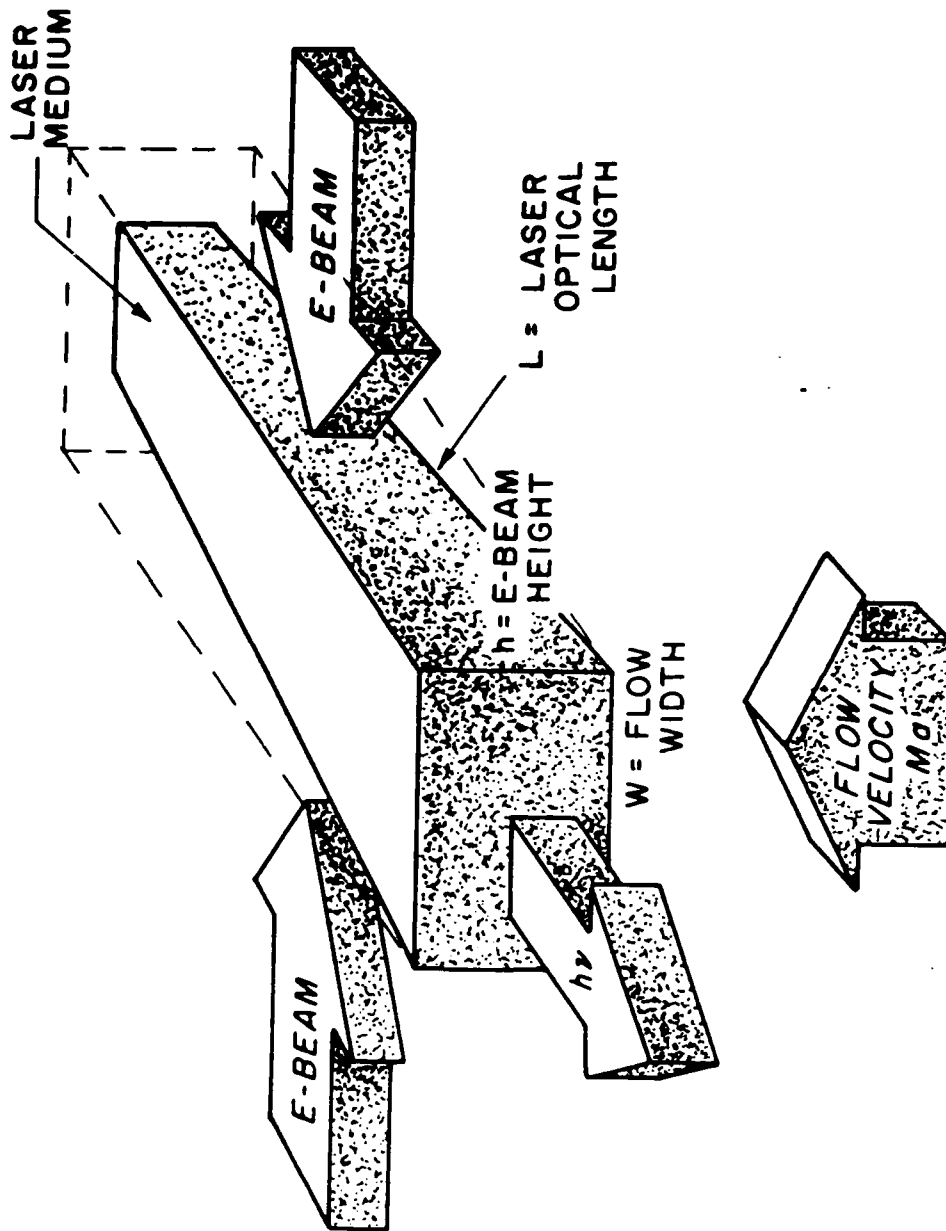


Figure 1.2: Expanding Wave Laser Amplifier Geometry

concepts developed for rectilinear architectures.

Efficient scaling to large energies from a single aperture has a number of advantages including:

- Simplification of Raman beam combining architecture
- Operation at lower pulse repetition rates for a given average power
- Reduction in fabrication cost for given laser output energy and power

Raman beam combining will be simplified because operation with higher single pulse energy per beam will require fewer excimer beams to reach the same energy level. This will significantly reduce the number of optical elements and complexity.

For high average power devices, operation at lower repetition rates and higher single pulse energies reduces foil cooling requirements and can lead to higher electron beam transmission through the foil support structure and therefore increased efficiency and reduced system cost. Lower repetition rates also reduce vacuum system requirements because the outgassing rates from the anode-cathode and foil support structures are strongly dependent on the average current density. These considerations, taken together, could allow the use of simpler, more rugged cold cathodes.

The design and construction of a small scale proof-of-principle experiment is described in Chapter 3. A XeCl excimer laser oscillator-amplifier system which was pumped by a single electron beam was built as a portion of this work. Details of the pulsed high voltage power supply, unstable resonator optics and other details are discussed. Chapter 4 presents the experimental results in which the actual experimental arrangement and calibration procedures are discussed. Finally, measurements of the extraction efficiency for collimated, one-dimensionally expanding (cylindrical), and two-dimensionally expanding (spherical) beams are shown. These measurements show clearly that the expanding wave laser concept leads to dramatically improved energy extraction at high flux levels.

As a convenience to the reader we include a reprint of a relevant paper, "Expanding Beam Concept for Building Very Large Excimer Laser Amplifiers," by J.H. Jacob, M.

Rokni, R.E. Klinkowstein, and S. Singer which was published Applied Physics Letters
(February, 1986).

CHAPTER 2

PERFORMANCE OF EXPANDING WAVE LASER AMPLIFIERS

2.1 INTRODUCTION

The energy extraction efficiency obtainable from conventional lasers and amplifiers with nonsaturable intrinsic absorption decreases substantially in cases in which the laser intensity is amplified to a level several times the saturation intensity.⁽¹⁻³⁾ This result is due to the fact that high intensities in the amplifier cause saturation of the small signal gain but not the absorption. In this chapter a new scalable amplifier concept. It was investigated under this contract, is analyzed. It maintains near-optimum extraction efficiency as the laser length increases beyond absorption-length products of one.

2.2 COMPARATIVE ANALYSIS OF EXPANDING WAVE AMPLIFIERS AND CONVENTIONAL AMPLIFIERS

The amplification in a one-dimensional laser amplifier is described by:

$$\frac{d\phi}{dx} = \frac{g_0\phi}{1+\phi} - \alpha_0\phi \quad (2.1)$$

where g_0 is the small signal gain, α_0 is the nonsaturable absorption coefficient and $\phi = I/I_s$ is the local optical intensity in units of the saturation flux. The denominator in the first term is due to gain saturation. At high fluxes the gain becomes a linear function of the coordinate rather than an exponential function.

The extraction efficiency of such an amplifier is defined by:

$$\eta_{extr} = (\phi_0 - \phi_i)/\phi_{avail} \quad (2.2)$$

where ϕ_i and ϕ_0 are the input and output fluxes respectively and ϕ_{avail} is the maximum available flux which is given by:

$$\phi_{avail} = N^*h\nu L/(\tau I_s) = g_0L \quad (2.3)$$

where N^* is the population inversion, τ is the excited state lifetime, $h\nu$ is the laser photon energy and L is the amplifier length. Hence;

$$\eta_{extr} = (\phi_0 - \phi_i)/g_0L \quad (2.4)$$

Integrating Eq. (2.1) for given values of g_0 , α_0 and ϕ_i , η_{extr} can be calculated as a function of amplifier length. Figures 2.1 and 2.2 show plots of η_{extr} as a function of amplifier length for values of ϕ_i of 0.1 and 1.0 using a small signal gain g_0 of 0.02 cm^{-1} and a g_0/α_0 of 7. At an injection level of $\phi_i = 0.1$, the extraction efficiency initially improves as the amplifier is lengthened, reaches a maximum value of 30% at about 4.5 meters and then decreases with further increases of the length. For an injected level of $\phi_i = 1.0$ the maximum extraction efficiency reaches a higher value (38%) at an amplifier length of 1.5 meters. This behavior may be understood if a local extraction efficiency⁽²⁾ is defined as:

$$\eta_{extr}(local) = \Delta\phi/\Delta\phi_{avail} \quad (2.5)$$

where $\Delta\phi_{avail} = g_0 \Delta x$ is the flux available for extraction along the incremental path Δx . Substituting from Eq. (2.1) we obtain:

$$\eta_{extr}(local) = \frac{1}{g_0} \frac{\Delta\phi}{\Delta x} = \frac{\phi}{1 + \phi} - \frac{\alpha_0\phi}{g_0} \quad (2.6)$$

From Eq. (2.6) an optimum local flux density can be found for which the local extraction efficiency reaches a maximum. This is a local value, not the integrated efficiency given by Eq. (2.4). The local optimum flux density is

$$\phi_{opt} = (g_0/\alpha_0)^{1/2} - 1 \quad (2.7)$$

and the maximum local extraction efficiency is given by:

$$\eta_{extr}(max) = [1 - (\alpha_0/g_0)^{1/2}]^2 \quad (2.8)$$

If the local flux density could be fixed at ϕ_{opt} as the beam is amplified, the integrated extraction would be the maximum possible. Since the local flux in a conventional rectangular geometry amplifier is a monotonic function of the amplifier length, the optimum flux,

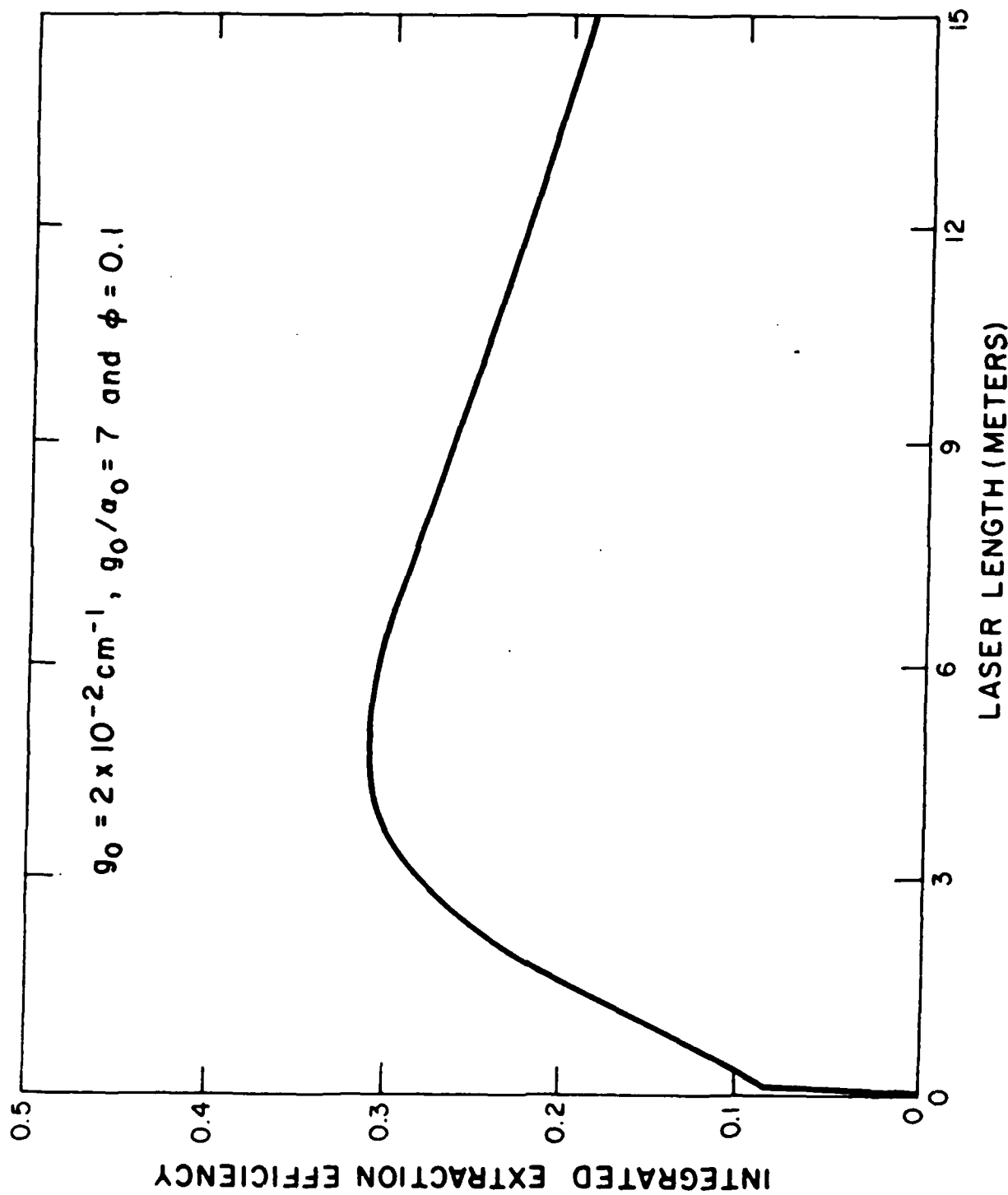


Figure 2.1: Extraction Efficiency as a Function of Amplifier Length for a Conventional Rectangular Amplifier and $\phi_{in} = 0.1$

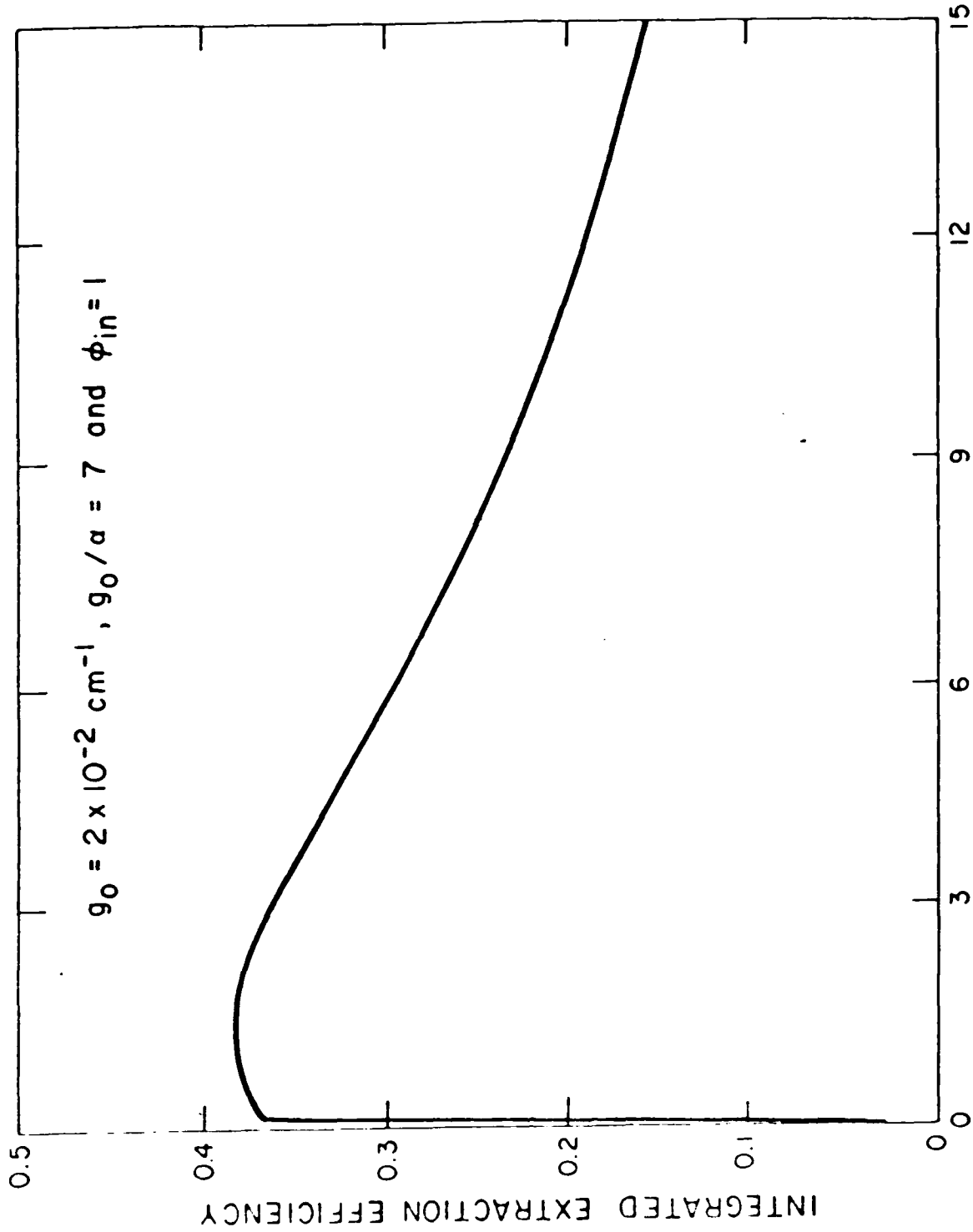


Figure 2.2: Extraction Efficiency as a Function of Amplifier Length for a Conventional Rectangular Amplifier and $\phi_{in} = 1.0$

given by Eq. (2.7), may be achieved over only a limited region of the amplifier. Therefore, for a particular g_0 and g_0/α_0 , there will exist an optimum laser amplifier length for most efficient integrated energy extraction.

Scaling a laser amplifier to large single pulse energies and maintaining an extraction efficiency close to the maximum locally achievable value requires that the local flux density be as near the optimum value over as large a region of the amplifier as possible. This can be achieved by using the amplifier in an expanding beam geometry as shown schematically in Fig. 2.3. The beam expansion is designed to compensate for the increase in flux created by the gain in the active medium. The beam expansion can be two-dimensional (spherical) or one-dimensional (cylindrical) with the expansion angle selected to maximize the extraction efficiency for a desired amplifier length.

To facilitate optimum design of laser amplifiers using the expanding beam concept, an amplifier model which can be solved numerically has been developed. As will be shown, in such a model an informative dependent variable is the total power $\psi(x) = \phi(x) \cdot S(x)$ flowing through the laser cavity. Here the beam cross sectional area at a location x is given by $S(x)$. The changing beam area requires an additional term in Eq. (2.1):

$$\frac{d\phi}{dx} = \frac{g_0\phi}{1+\phi} - \alpha_0\phi - \frac{\phi}{S(x)} \frac{dS}{dx} \quad (2.9)$$

Substituting for the laser power reduces Eq. (2.9) to the simpler form:

$$\frac{d\psi}{dx} = \frac{g_0\psi}{1+\psi/S} - \alpha_0\psi \quad (2.10)$$

Comparing Eq. (2.10) with Eq. (2.1) it is clear that expanding the beam is equivalent to increasing the saturation power along the length of the device.

The extraction efficiency in this case is given by: $\eta_{extr} = (\psi_0 - \psi_i)/\psi_{avail}$ where ψ_0 and ψ_i are the output and input powers (in units of I_s times the local area) respectively and ψ_{avail} is the available power given by:

$$\psi_{avail} = \frac{N^*}{\tau} \frac{h\nu V}{I_s} = g_0V \quad (2.11)$$

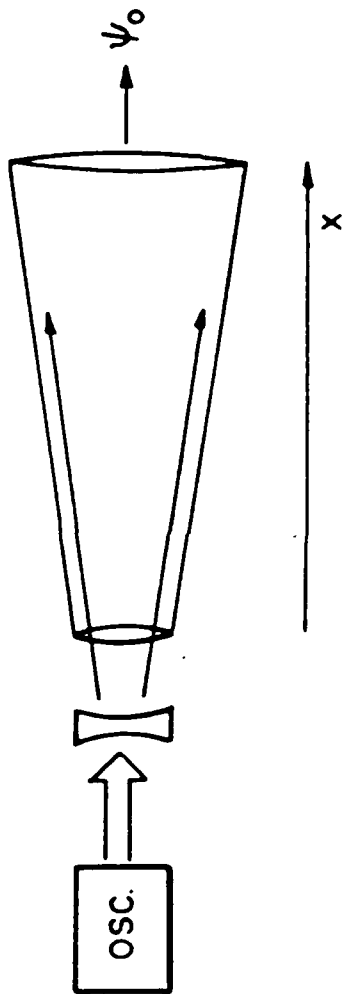


Figure 2.3: Schematic Geometry of an Expanding Wave Laser Amplifier

where V is the volume of the amplifier from which the beam extracts energy.

Equation (2.10) must be solved numerically for a given set of amplifier parameters. From these results the area expansion ratio $S(L)/S(0)$ can be found which maximizes the extraction efficiency for a given length.

In Figures 2.4 through 2.6 the dependence of the integrated extraction efficiency as a function of amplifier length for an expanding beam amplifier is compared with that of a conventional amplifier. The expanding wave amplifier is modelled as having a square optical angle of $\theta = 5^\circ$, and an entrance area of $S_0 = 10^3 \text{ cm}^2$. The plots correspond to ϕ_i values of 0.1, 1 and 1.5 a small signal gain of $g_0 = 0.02 \text{ cm}^{-1}$ and a gain to loss ratio (g_0/α_0) of 7. From these figures, the improvement in the integrated extraction efficiency at large lengths, obtained by using the expanding beam concept, is obvious. For the largest lengths of 15 meters, the expanding wave amplifier provides an extraction efficiency of twice that of the conventional rectilinear amplifier.

These results indicate that for a gain medium with nonsaturable intrinsic absorption, the expanding wave geometry allows length scaling of laser amplifiers while maintaining integrated extraction efficiencies close to the maximum local value. The expanding wave technique also permits considerably improved extraction for a fixed amplifier length as shown in Fig. 2.7. The amplifier in this situation is modelled to be 50 cm long. A small signal gain of 0.02 cm^{-1} and a gain to loss ratio of 7, characteristic of XeCl pumped by an electron beam, were assumed.

For the unexpanded beam case, the extraction efficiency increases rapidly as the input flux increases and reaches a peak of 38% for an input flux of $1.5 \phi_s$. The extraction efficiency then decreases and reaches zero for an input of $6 \phi_s$. This situation follows from Eq. (2.1) when the injected level is $\phi_i = (g_0/\alpha_0 - 1)$ the right hand side vanishes identically. At this flux level, the saturated gain provided by the active medium is precisely equal to the nonsaturable absorption loss and no net gain occurs. At higher injected flux levels the loss dominates over the gain and a net loss to the beam takes place.

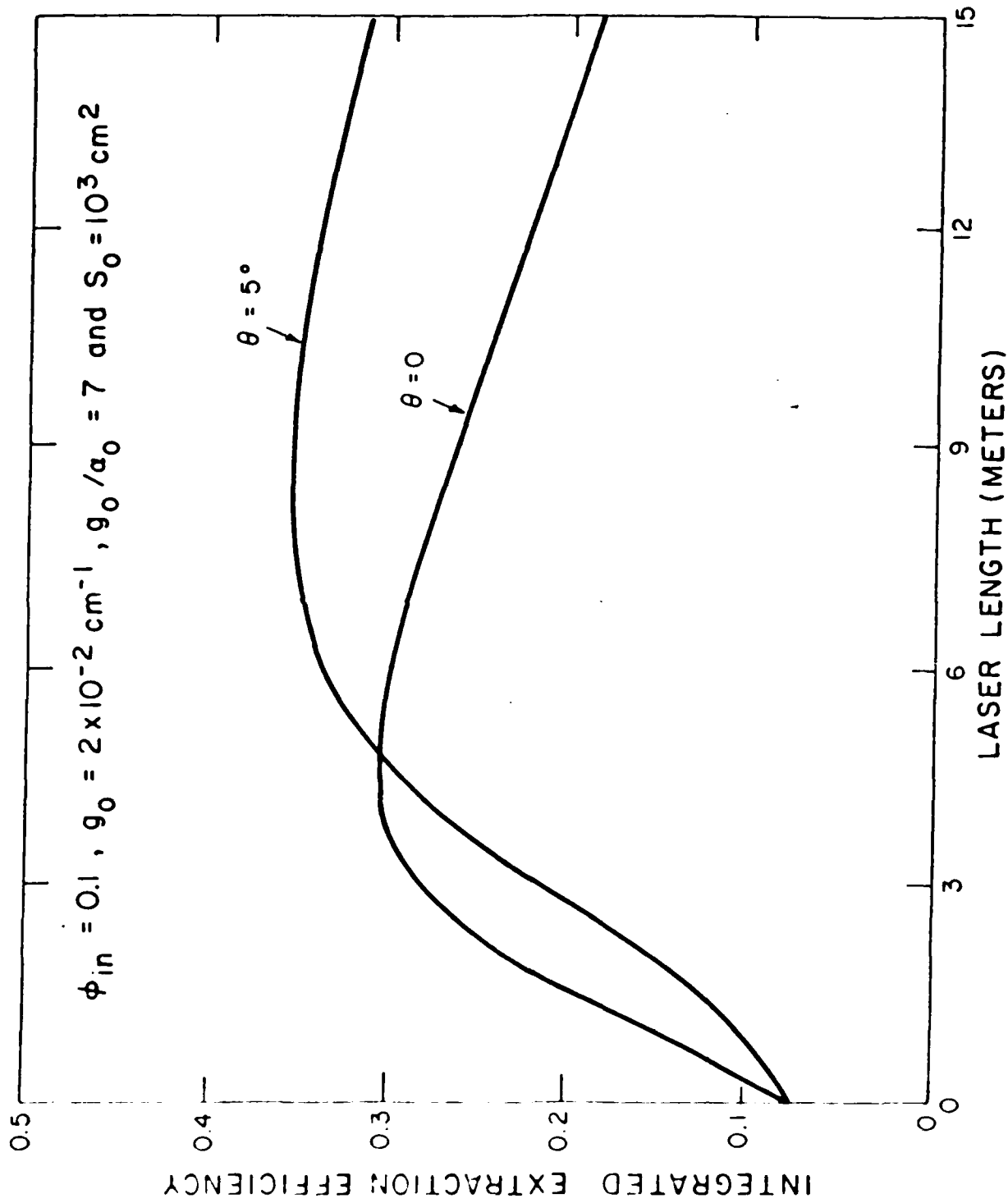


Figure 2.4: Comparison of Integrated Extraction Efficiency of Expanding and Collimated Beams for $\phi_{in} = 0.1$

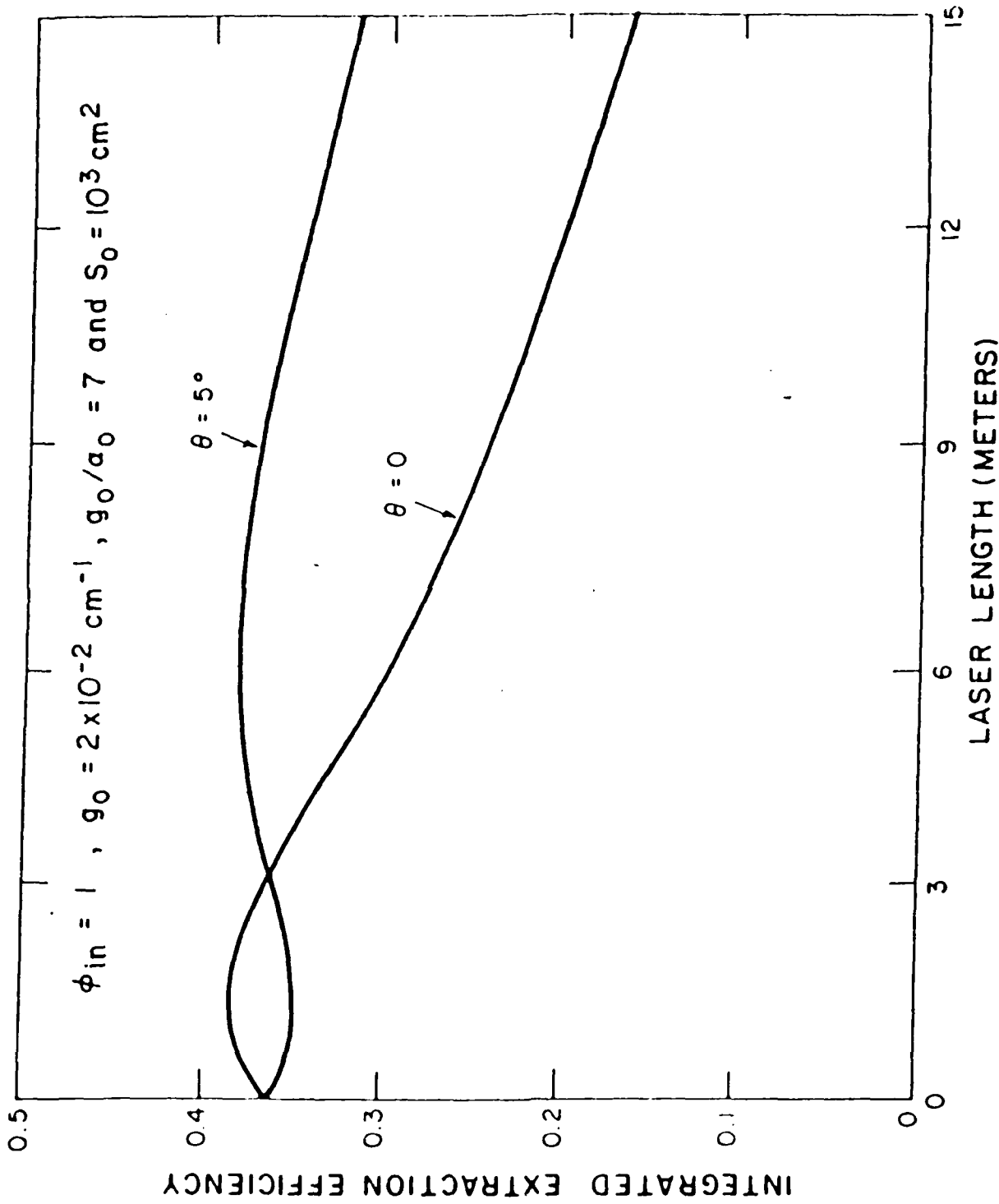


Figure 2.5: Comparison of Integrated Extraction Efficiency of Expanding and Collimated Beams for $\phi_{in} = 1.0$

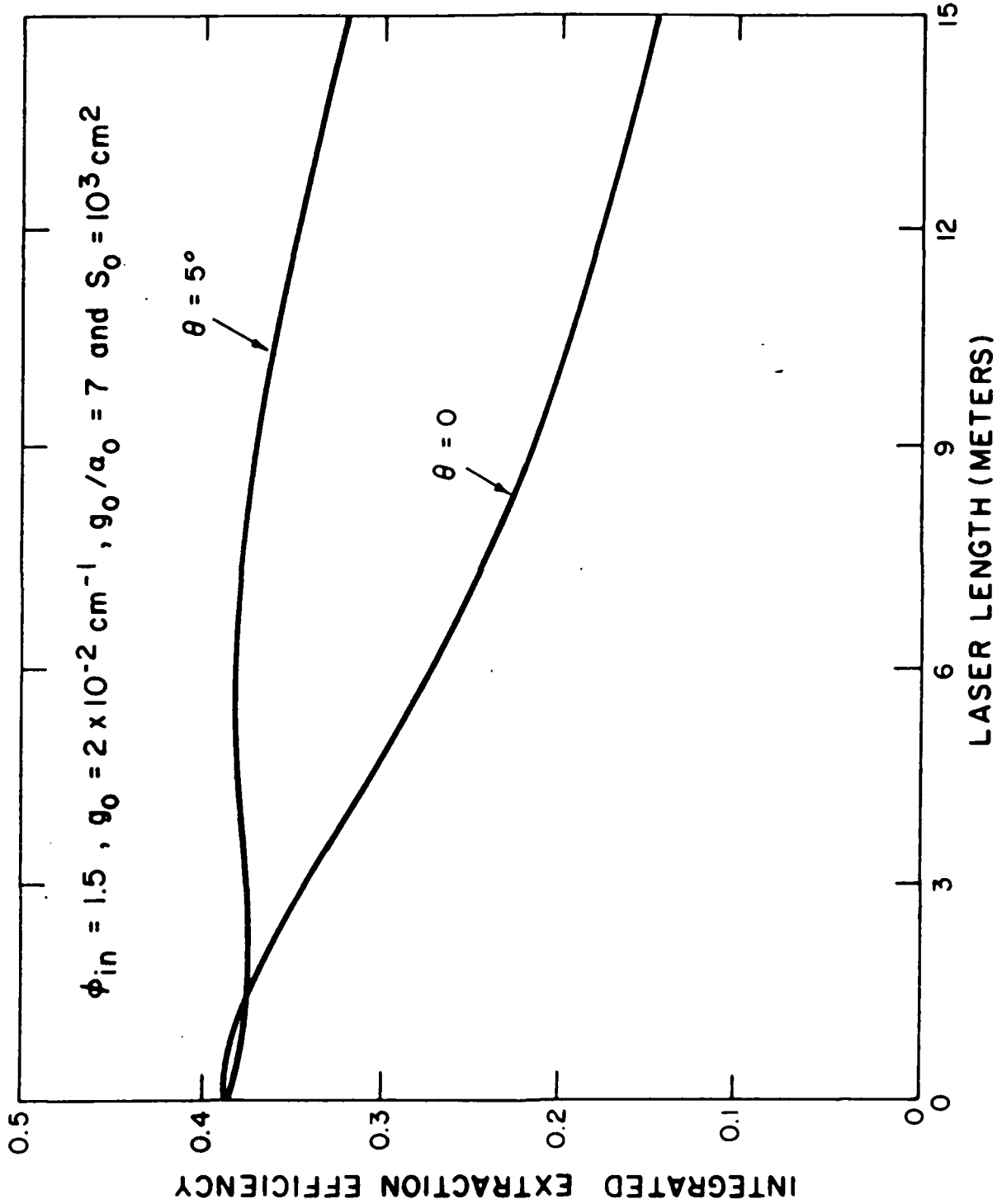


Figure 2.6: Comparison of Integrated Extraction Efficiency of Expanding and Collimated Beams for $\phi_{in} = 1.5$

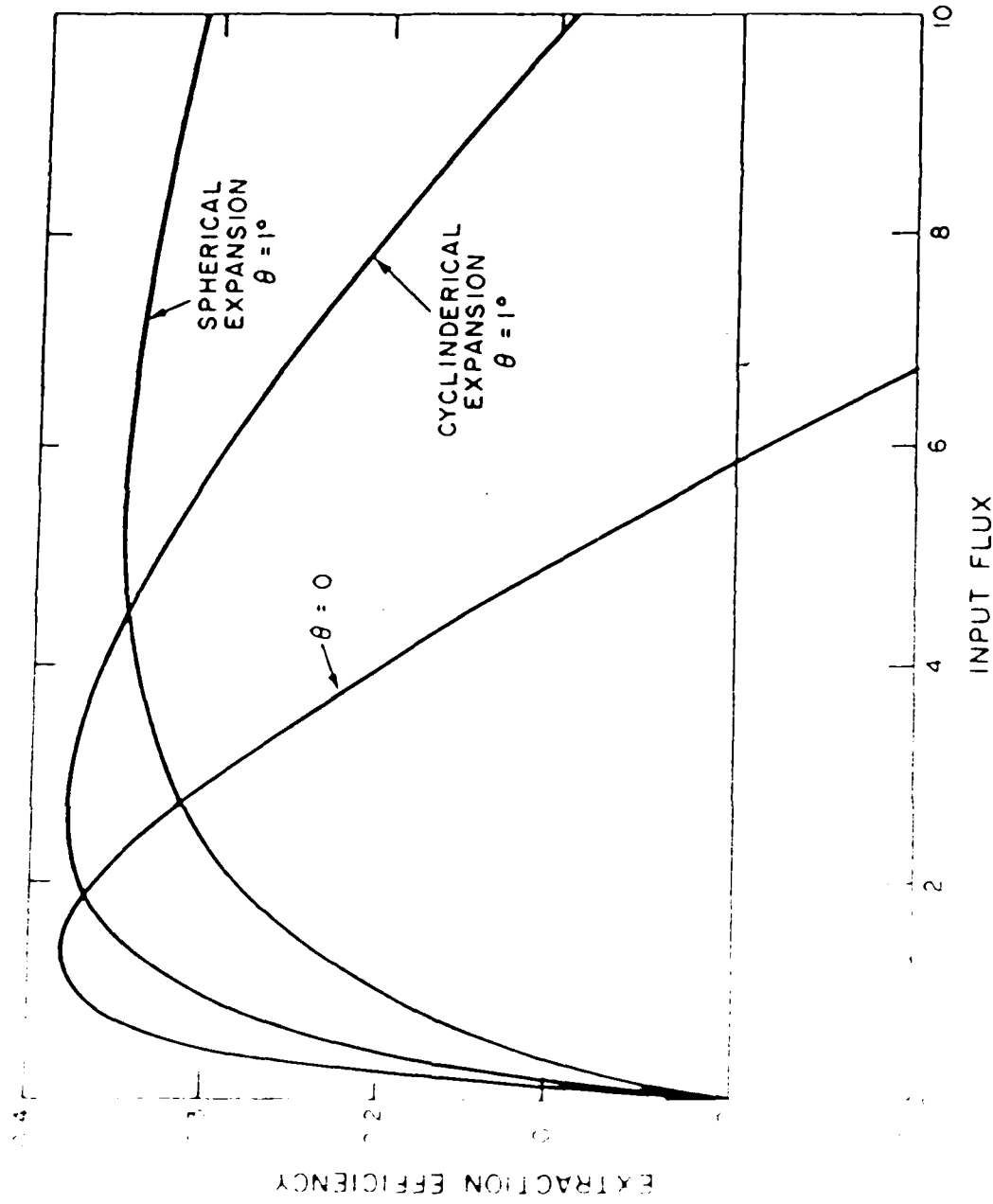


Figure 2.7: Extraction Efficiency at Fixed Amplifier Length for Collimated, Cylindrical, and Spherical Expansion. Laser Parameters are: $g = .02 \text{ cm}^{-1}$, $g/\alpha = 7$ and Laser Length = 50 cm. **SCIENCE RESEARCH LABORATORY**

The second curve in Fig. 2.7 displays dramatically different behavior. As the input flux is increased, the efficiency rises more slowly and reaches a peak of 35% when $\phi_i = 5$. At this level the extraction from the nonexpanded beam approaches zero. The cylindrical expansion falls between these two cases. These results suggest that the expanding beam concept may be verified simply in a fixed length amplifier by measuring the extraction efficiency over a range of input fluxes for collimated and expanding beams.

CHAPTER 3

PROOF-OF-PRINCIPLE EXPERIMENT

3.1 INTRODUCTION

To verify the expanding beam laser concept for scaling laser amplifiers, a small scale proof of principle experiment has been designed and constructed. A single-sided electron beam pumped volume (11 cm × 11 cm × 100 cm) served as a master oscillator and simultaneously as a power amplifier as shown in Fig. 3.1. The upper half of the pumped volume was configured as an oscillator which employed unstable resonator optics to generate an output beam of adequate quality. A 3.8 cm diameter portion of the output beam was reduced in area by a telescope and injected into the lower amplifier section. This reduction in beam size was used to conveniently reach proper injected flux levels. A gas absorber cell (containing a mixture of Cl₂ and Ar) permitted the injected flux level to be controlled while pumping the laser at constant conditions. Finally, a spherical or cylindrical lens could be inserted into the optical path to permit the variation in extraction efficiency of one- and two-dimensional expanding beams to be compared to that of a collimated beam.

3.2 PULSED POWER AND MAGNETIC FIELD DESIGN

A block diagram of the elements required to construct an electron beam pumped excimer laser system is shown in Figure 3.2. The laser oscillator was designed to provide 6 Joules of output in a 300 nsec pulse using a 10 × 6 cm² portion the laser cross section.

Assuming typical values for laser efficiency and allowing for the pumping of the additional cross section required for the amplifier section and losses in the foil and foil support structure a single sided electron beam must be capable of producing 10⁴ Joules/μsec in electron beam power. An electron beam energy of at least 250 kV is needed for adequate beam penetration and uniform energy deposition within the laser medium. From the electron beam power and energy the pulsed power supply output impedance may be found

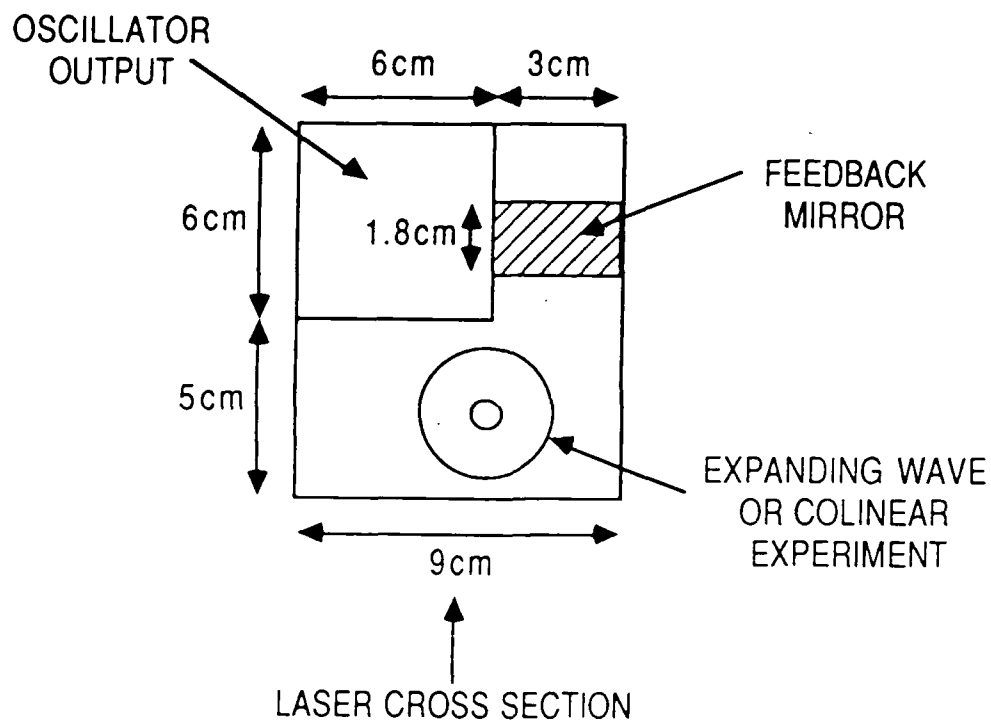


Figure 3.1: Laser Cross Section Showing Electron Beam Pumped Master Oscillator-Amplifier Configuration. The Electron Pumping Beam Enters From the Left.

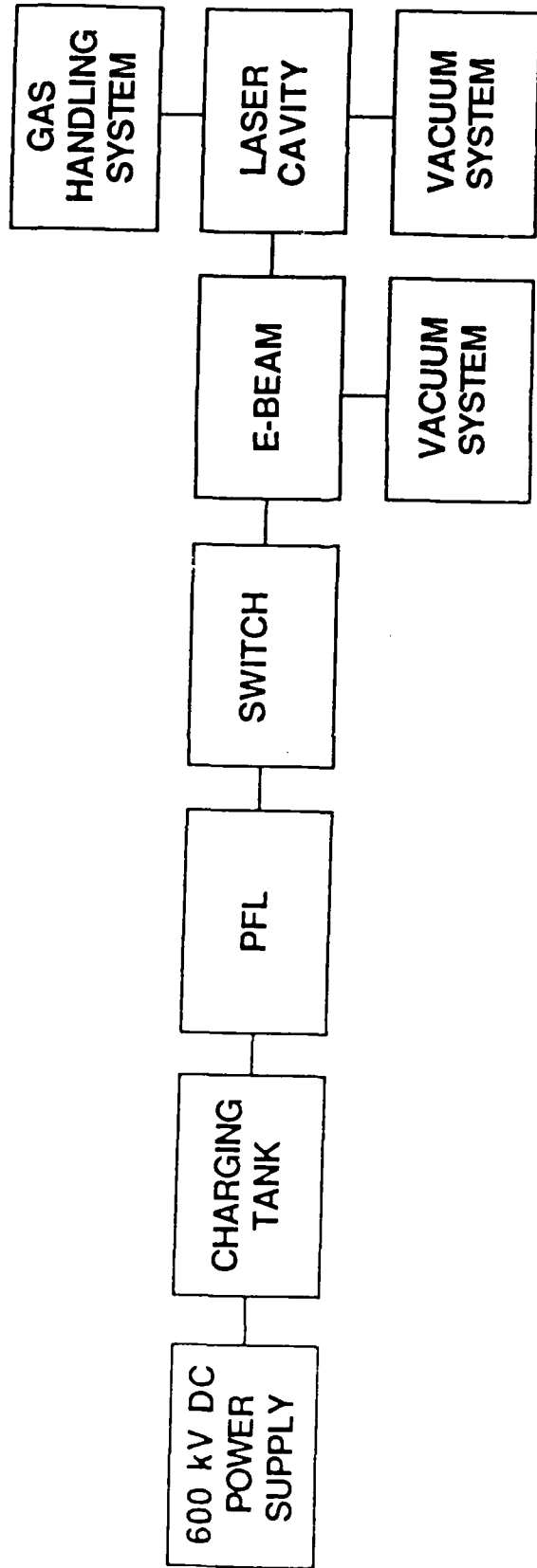


Figure 3.2: Block Diagram for Expanding Beam Laser Amplifier Proof-of-Principle Experiment.

from:

$$R = V^2/P = 6 \Omega \quad (3.1)$$

The electron beam requirements are summarized in Table 3.1. A pulsed power system consisting of a 600 kV, 1 milliamp direct current power supply which charges seven cables in parallel was selected because of its operational simplicity and reliability. A cable system combines energy storage and the functions of a pulse forming line into a single device. The cables use an oil impregnated dielectric and are rated to 1 MV DC. At 500 kV charging voltage a total of 4.75 kJ is stored in the cable system. The cable lengths were selected to generate a 400 nsec output pulselength. Figure 3.3 shows the achieved waveforms of current (measured by a calibrated Rogowski loop) and cathode voltage (measured by calibrated capacitive probe). The desired magnitudes of current and voltage (13 kA, 240 kV) along with a 50 nsec risetime are evident. Comparison of the current measured at the cathode to that which flows through the drift space allows the transparency of the anode to be estimated at 65%. The anode screen itself has a geometric transparency of 70%.

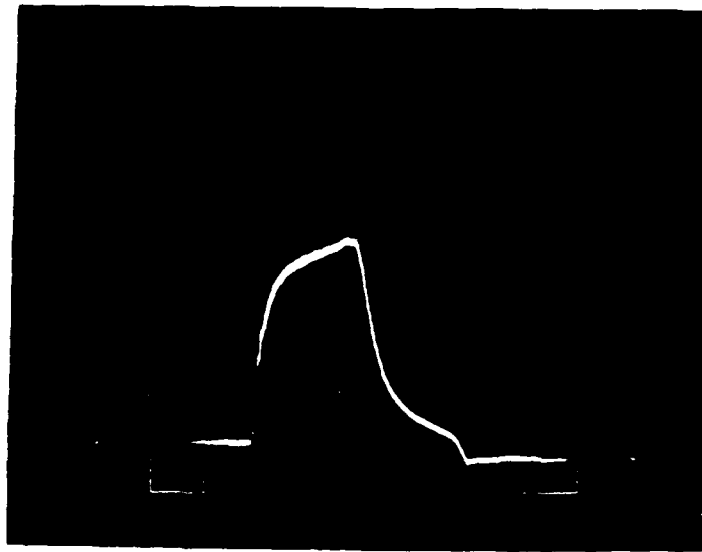
This configuration requires only a single trigatron high voltage switch to transfer the energy stored in the cables into the electron beam system. This approach eliminates jitter problems due to multiple spark gaps. An important design issue in such a system is the high voltage terminations at the ends of the charge. Since half the charge voltage appears at the cathode for a properly matched system, the terminations must be designed to withstand 600 kV DC with adequate safety margins. A numerical electrostatic potential solver was employed to verify that the maximum electric field stresses within the termination were limited to acceptable levels. Figure 3.4 shows the equipotentials in a critical region of the termination design. The maximum field stress at full voltage is $\sim 60\text{kV/cm}$ which is a factor of 2 below the point at which flashover along the surface of the lucite insulator would start to become a problem. A photograph of a complete cable and termination assembly is shown in Fig. 3.5.

Guide magnetic field coils are required to prevent the self field of the electron beam

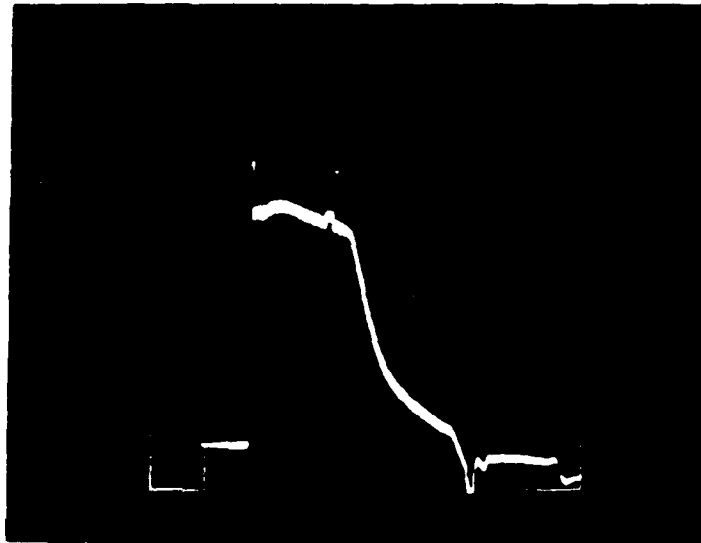
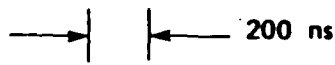
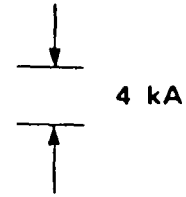
TABLE 3.1:

Electron Beam System Requirements

— IMPEDENCE	6 Ω
— E-BEAM VOLTAGE	250 kV
— E-BEAM CURRENT	40 kA
— CATHODE AREA	11 X 100 cm ²
— CURRENT DENSITY	36 A/cm ²
— ANODE/CATHODE SPACING	5 cm
— PULSE LENGTH	4 x 10 ⁻⁷ cm



CURRENT



VOLTAGE

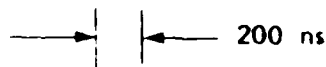
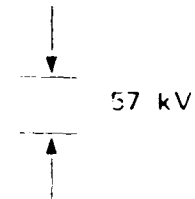


Figure 3.3: Electron Beam Current and Voltage

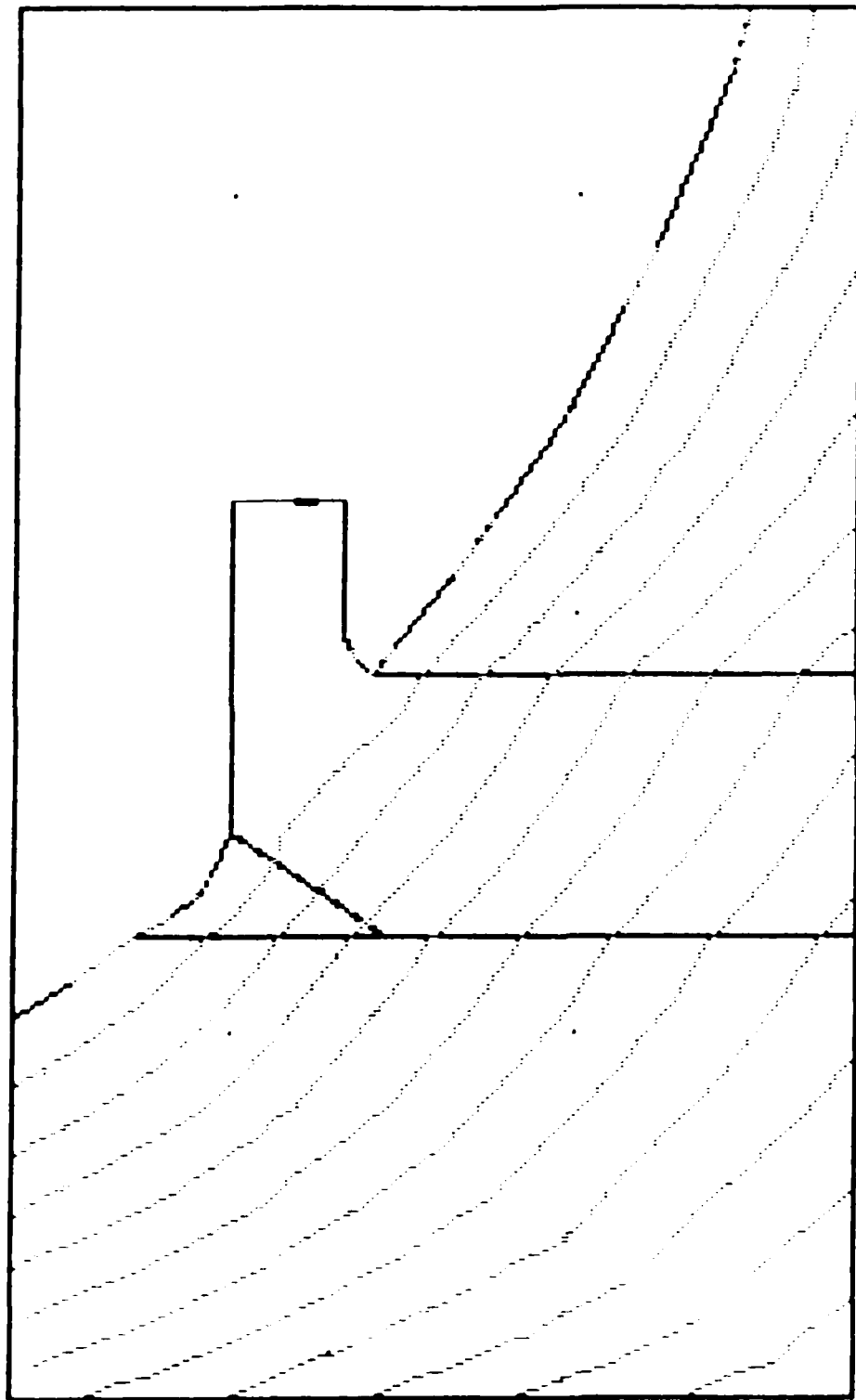
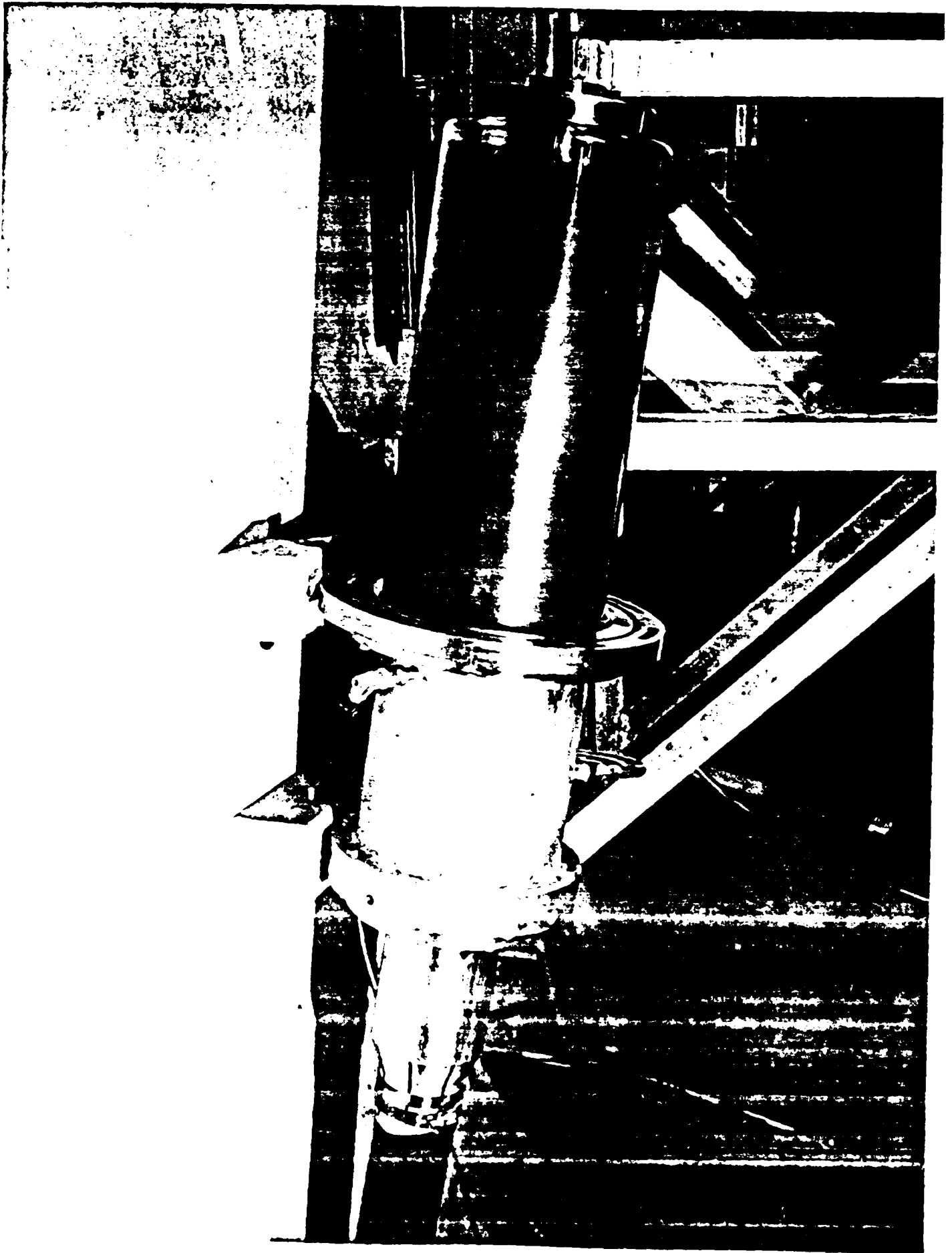


Figure 3.4: High Voltage Termination Equipotentials in Highest Electric Stress Region. Equipotentials Shown at Every 30 kV.



from pinching the current and leading to nonuniform pumping or foil damage. A guide field also limits scattering of the electron beam out of the laser cavity by the laser gas mixture. The field strength required to prevent pinching may be estimated by modelling the 11 cm × 100 cm electron beam as an infinite current sheet. The strongest self-field is located at the midpoint of the long axis of the current distribution. Ampere's law⁽⁴⁾ can be used to derive:

$$B_{long} = \frac{\mu_0 I h}{2} \quad (3.2)$$

where μ_0 is the permeability of free space, I is the beam current density, and h is the height of the cathode. At a beam current of 40 A/cm² Eq. (3.2) results in a self-field of ~ 250 Gauss. Corrections due to the finite width of the cathode raise this value by ~ 10%. Two racetrack magnetic field coils are used to generate a uniform 2000 G guide field along the electron beam. Field uniformity was evaluated using SRL MAG-PC software and was designed to be better than 4% within the pumped volume of the laser. Each 2.4 meter × 0.72 meter water cooled coil carries ~ 1200 amperes at a 2000 G field.

3.3 LASER OSCILLATOR RESONATOR DESIGN

An important issue which must be addressed in the design of this experiment is a suitable laser system. Shown in Table 3.2 are three candidate excimer lasers (XeF, XeCl and KrF). An acceptable balance between lasing efficiency and required flux level is provided by XeCl. Although KrF is more efficient, the combination of a high saturation flux and high gain to loss ratio raises the required laser output to unacceptable levels.

An unstable optical resonator⁽⁵⁾ is an appropriate choice to generate a near diffraction limited output beam in a large volume, high gain laser such as XeCl. The output flux from a laser oscillator may be predicted by using the analysis of Rigrod⁽²⁾.

$$\phi_{osc} = \frac{(g_0 - \alpha_0)L \cdot \ln \sqrt{r}}{1 - \alpha_0 L / \ln \sqrt{r}} \quad (3.3)$$

where ϕ_{osc} is the output flux density in units of the saturation flux and r is the cavity roundtrip feedback. For the pump conditions anticipated $g_0 = 0.06 \text{ cm}^{-1}$ and $g_0 / \alpha_0 = 6$

TABLE 3.2:
Properties of Candidate Excimer Laser Systems

EXCIMER LASER	WAVELENGTH nm	g/a	SATURATION FLUX ϕ_s kW/cm ²	REQUIRED FLUX $> \phi_s (g/a - 1)$ MW/cm ²	INTRINSIC EFF
XeF	350	10	300	2.7	2.5
XeCl	308	7	500	3.0	7
KrF	250	15	1000	14	10

These values lead to:

$$\phi_{osc} = 2.06 \quad \text{at} \quad r = 0.10 \quad (3.4)$$

Therefore, a resonator with a 10% feedback will generate an output beam with a flux density of 2.06 times the saturation flux. This corresponds to an extraction efficiency from the oscillator of 34%. The optimum of Eq. (3.3) with respect to the feedback occurs at $\phi_{osc} = 2.10$ and $r = 0.055$. The additional feedback of a 10% feedback design allows a margin for losses in coatings, etc. A confocal design is used to produce a collimated output beam. The feedback mirror is offset to allow a unobstructed 6×6 cm beam to exit the cavity. Output energies of 6 - 7 Joules have been extracted from the oscillator section of the laser.

A photograph of the assembled laser system is shown in Fig. 3.6. The racetrack magnetic field coils and cable pulsed power supply are evident.

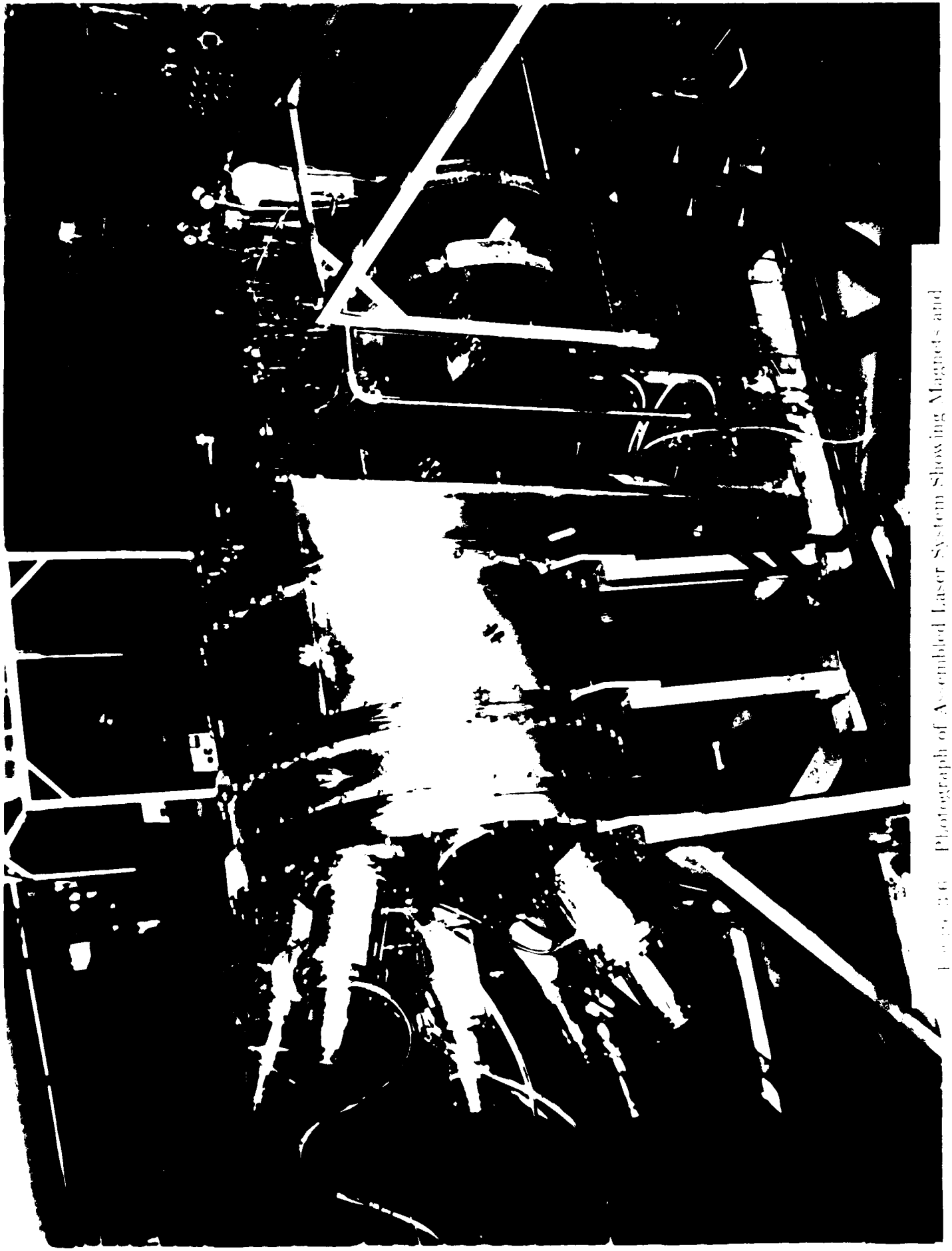


Figure 3.6 Photograph of Assembled Laser System Showing Magnets and Cable and Pulled Power Supply

CHAPTER 4

EXPERIMENTAL RESULTS

4.1 INTRODUCTION

The energy extraction of an XeCl laser amplifier using collimated and expanding beams was measured. The predicted improvement in extraction by the use of an expanding wave amplifier was observed.

4.2 LASER DIAGNOSTICS

The performance of the electron beam system was monitored by a calibrated capacitive high voltage probe and calibrated Rogowski loops. The high voltage probe was calibrated by generating a high voltage pulse at the cathode and comparing the capacitive probe signal to a calibrated Tektronix Corporation Model P6015 high voltage probe. This was performed with the electron beam box in normal operating position. Access to the cathode was achieved by removing the anode, foil, and foil support. High current carbon surge resistors were used to simulate the 6 Ω diode impedance. The maximum calibration voltage was limited by the calibrated probe to 40 kV. This voltage was low enough that no breakdown problems into air were observed. The Rogowski current probes were also calibrated in place using a Ion Physics Corporation Model CM-10-M current transformer to measure the current flowing in the surge resistors.

The optical layout is shown in Fig. 4.1. A gas absorber cell, which contained a mixture of Cl₂ and Ar was used to attenuate the output laser intensity to the proper level. Typically a 15:1 Ar to Cl₂ mixture was employed. Reducing the total pressure in the cell reduced the attenuation in controllable steps. A 3.8 cm diameter portion of the oscillator output beam was isolated by a mask and reduced in size by a 3.8:1 telescope to yield a 1 cm diameter beam which was used in the extraction experiments. A 3 degree fused quartz wedge reflected a small fraction of the beam onto a Hamamatsu R1193U

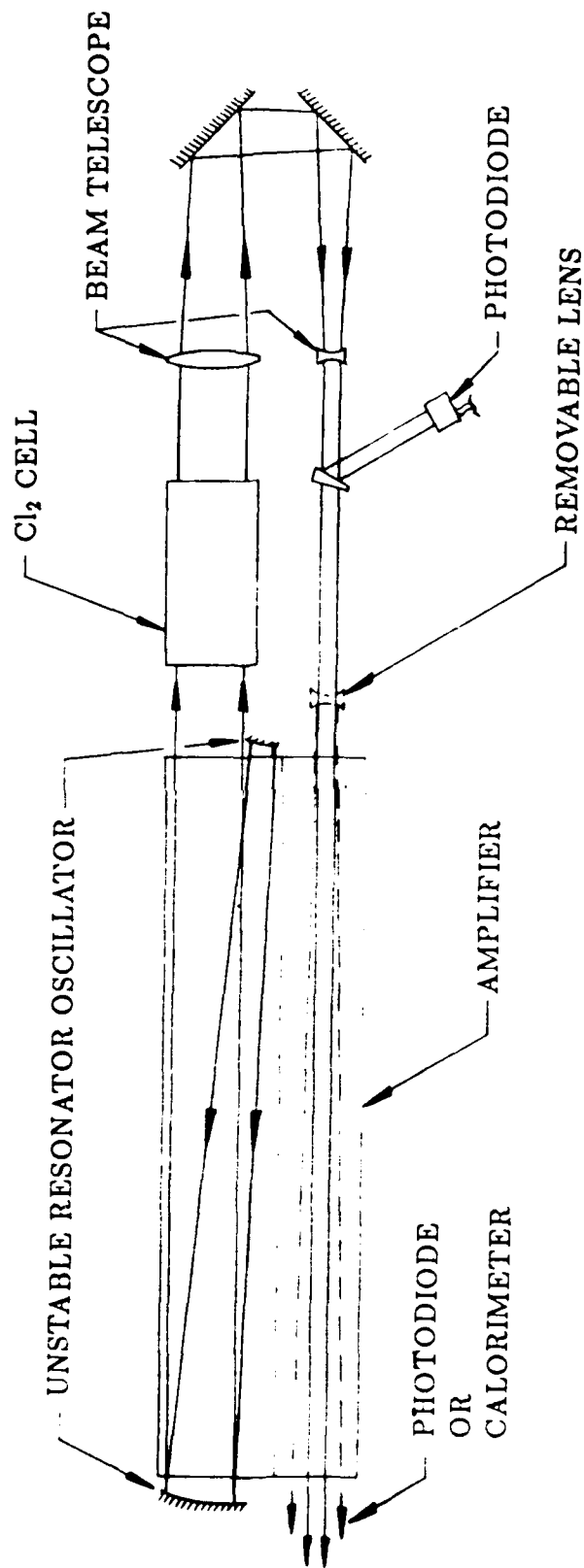


Figure 4.1: Optical Layout of the Expanding Beam Laser Amplifier Experiment.

photodiode as a monitor of the laser output. A second Hamamatsu photodiode (which had been calibrated relative to the first by using the XeCl laser) was used to record the amplified beam intensity. Both diodes had a well defined aperture. Laser energies were measured with a Scientech Corporation volume absorbing calorimeter. A typical laser shot is shown in Fig. 4.2 which displays the electron current flowing through the drift space, the cathode voltage, and the laser output pulse.

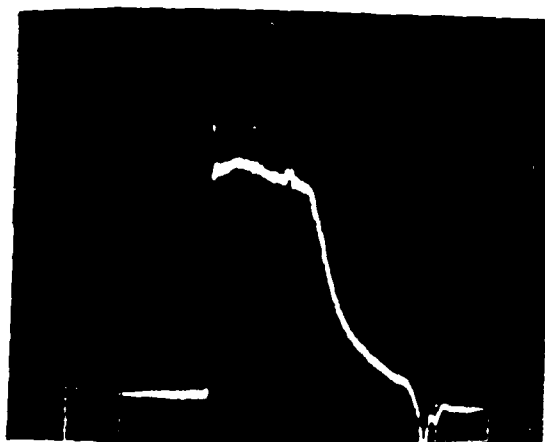
4.3 EXTRACTION MEASUREMENTS

Energy extraction measurements were performed at the conditions shown in Fig. 4.2. The electron beam voltage was 240 kV and the current density was 13 A/cm². Adequate penetration across the cross section of the electron beam at this voltage was verified by a Monte-Carlo electron beam deposition code. The laser gas mixture included 2 torr HCl and 40 torr Xe per atmosphere. A total pressure of 1.15 atm with an Ar buffer was employed.

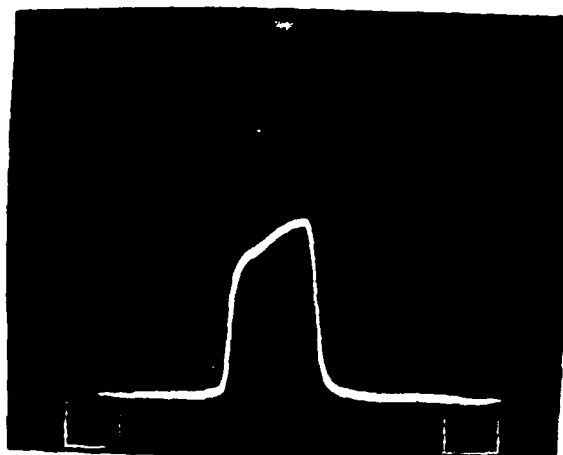
In Fig. 4.3 the extracted energy as a function of the input flux for a collimated beam is shown. The beam was verified to maintain a diameter of 1.0 cm (within less than 1 mm variation) over a 3 meter path in the laboratory. The zero crossing of the extraction when the injected flux level reaches high levels is evident. The solid curve is an analytic solution to the amplifier equation chosen to cross zero at the same place as the data and to fit the data at high injected fluxes. Values of $g_0 = 0.07 \text{ cm}^{-1}$ and $g_0/\alpha_0 = 6$ gave an acceptable fit to the data except at the lowest injection levels. These fitting parameters determine the injected flux scale, i.e. $\phi_{in} = 5\phi_s$ at an injected flux of one unit. The maximum injected intensity is approximately 4 MW/cm². Extrapolating from recent measurements⁽⁶⁾ such an intensity corresponds to a ϕ/ϕ_s of 13. The small signal gain of 0.07 cm^{-1} and $g_0/\alpha_0 = 6$ are consistent also with the AVCO data⁽⁶⁾ allowing for the present experimental conditions. A one-dimensional beam expansion is compared to the collimated case in Fig. 4.4. The same parameter values as were used in Fig. 4.3 were used to calculate the second theoretical curve. A significant improvement in extraction can be seen. For example, at an injected flux level for which a collimated beam extracts no net



(a) CURRENT
4.1 kA/div



(b) VOLTAGE
57 kV/div



(c) LASER OUTPUT



200 ns

Figure 4.2: Typical XeCl Laser Shot Showing (a) The Electron Beam Current Through the Drift Space, (b) The Cathode Voltage, and (c) The Laser Optical Output.

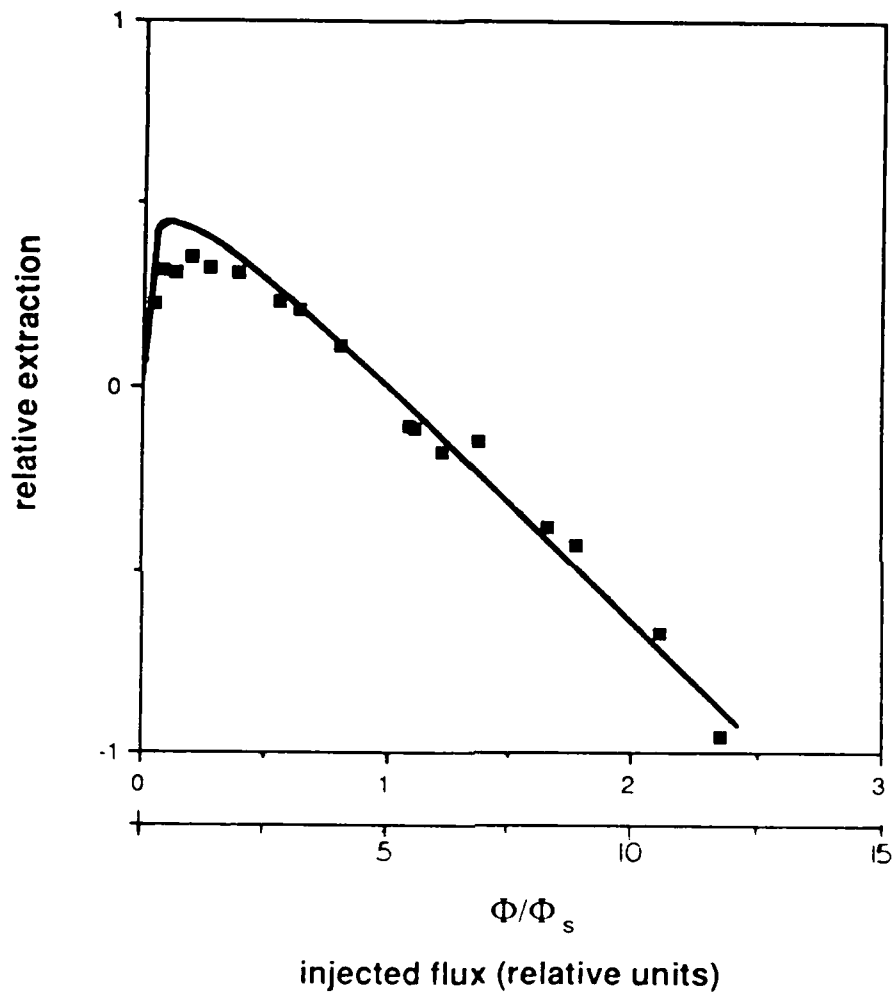


Figure 4.3: Measured Extraction Efficiency for a Collimated Beam as a Function of Input Flux Density.

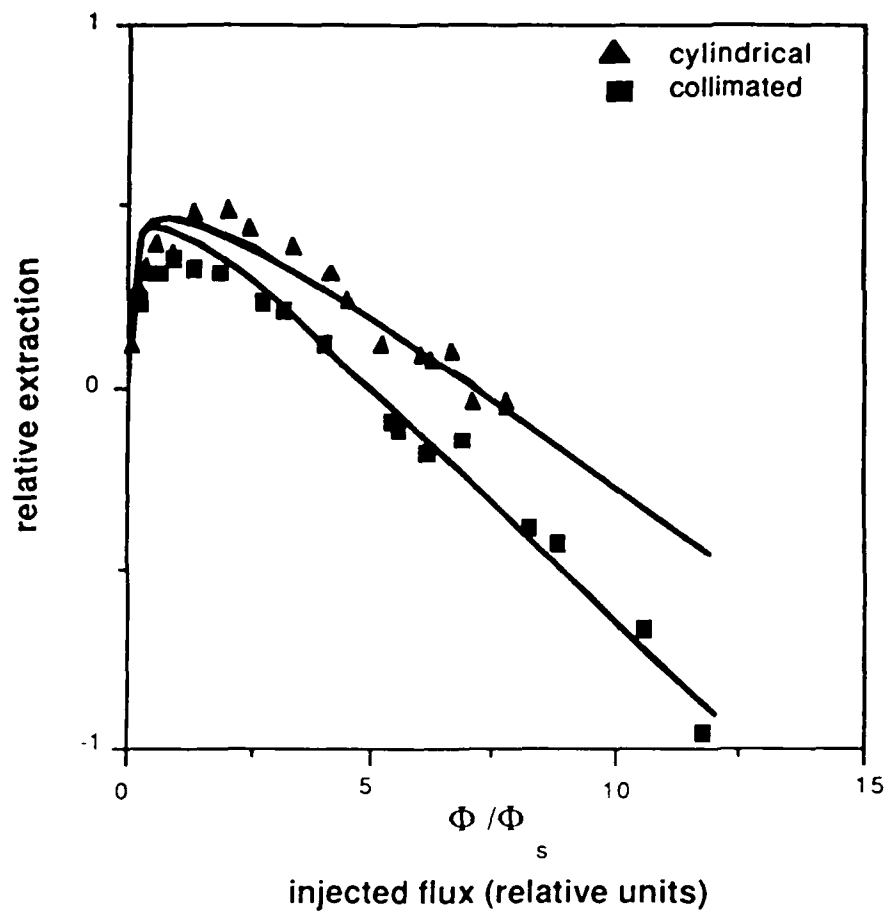


Figure 4.4: Measured Extraction Efficiency of Cylindrically Expanding Beam Compared to Collimated Beam.

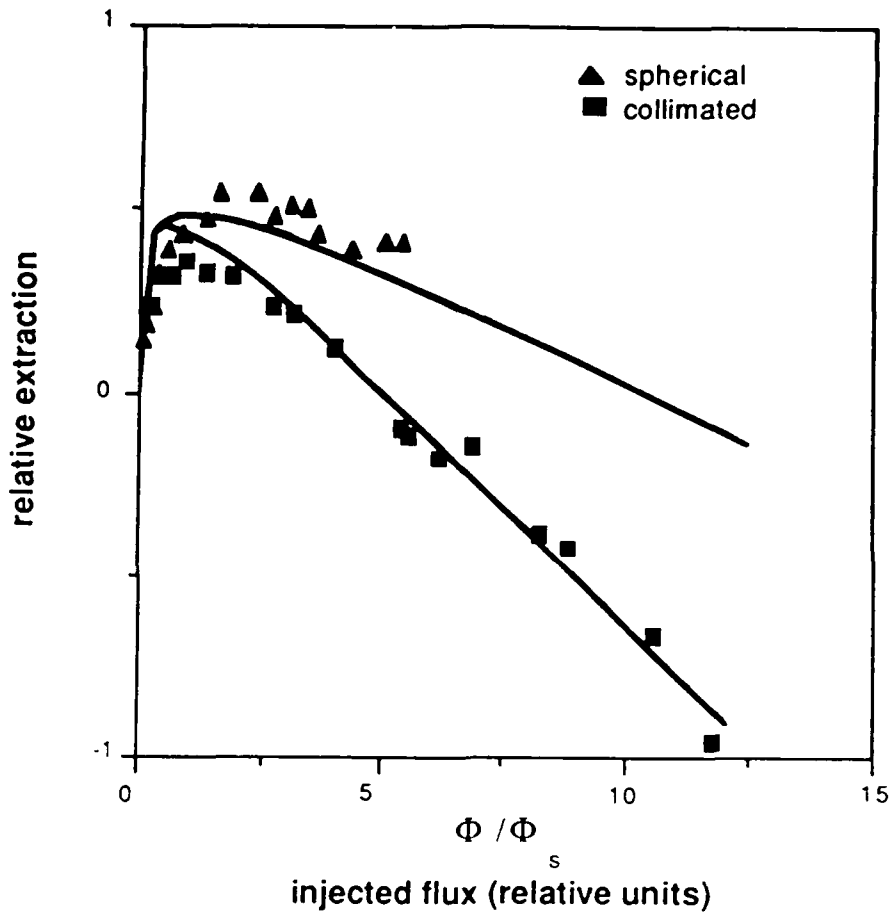


Figure 4.5: Measured Extraction Efficiency of Spherically Expanding Beam Compared to Collimated Beam.

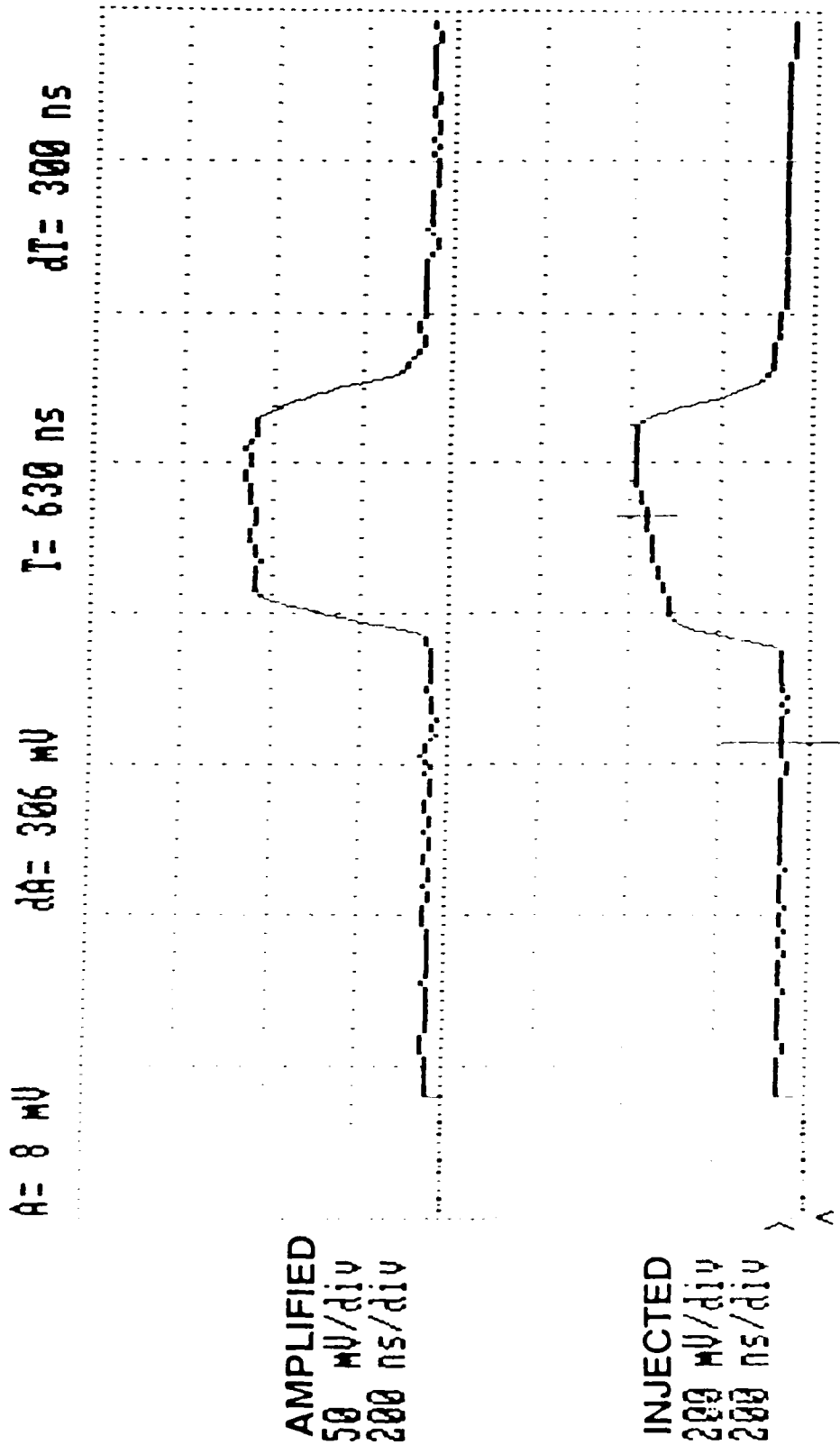


Figure 4.6: Photodiode Records of Laser and Amplifier Outputs (a) Amplified Collimated Beam and (b) Injected Beam.

A = 2 mV dA = 218 mV T = 710 ns dT = 300 ns

AMPLIFIED
100 mV/div
200 ns/div

INJECTED
100 mV/div
200 ns/div

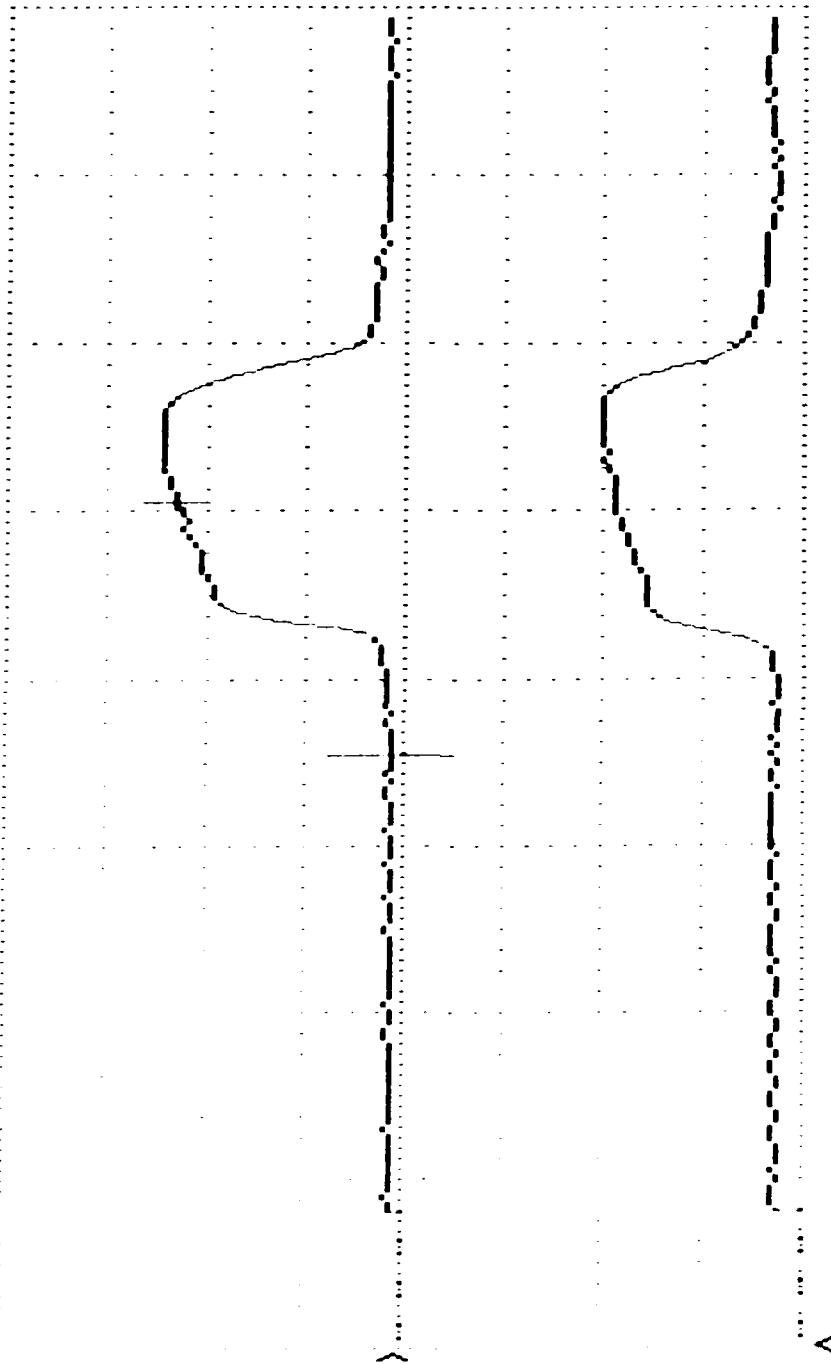


Figure 4.7: Photodiode Records of Laser and Amplifier Outputs (a) Amplified Expanding Beam and (b) Injected Beam.

energy this expanding beam still extracts energy at 65% of the peak extraction efficiency. The effect of a two-dimensional expansion is shown in Fig. 4.5. A negative lens of -100 cm focal length was used to produce the expansion in both cases. A cylindrical lens for Fig. 4.4 and a spherical lens for Fig. 4.5. Particularly dramatic is the improvement in the spherical expansion. For this spherical expansion the energy extraction remains at 74% of the peak value at an injected flux for which a collimated beam would not extract net energy. These plots are of relative efficiency, i.e. the extra volumes that the expanding beams interact with have been allowed for.

An additional verification that an expanding beam reduces the effects of gain saturation is shown in Figures 4.6 and 4.7. These figures show the time history of the two photodiodes as recorded by the data acquisition system. In each case the upper curve is the time history of the amplified laser pulse and the lower curve is the injected pulse shape. In Fig. 4.6 gain saturation causes the output pulse to be flattened. An expanded beam, shown in Fig. 4.7, follows the input shape and is not saturated. The optical attenuation used on the second photodiode was lower for the expanded beam data. The detected electrical signal was higher in this case indicating that saturation of the detector or electrical amplifiers is not occurring.

REFERENCES

1. See for example: M. Rokni, J.A. Mangano, J.H. Jacob, and J.C. Hsia, "Rare Gas Fluoride Lasers" IEEE J. Quantum Electron. QE - 14, 14, 464 (1978).
2. W.W. Rigrod, "Homogeneously Broadened CW Lasers with Uniform Distributed Loss", IEEE J. Quantum Electron, QE - 14, 377 (1978).
3. J.H. Jacob, M. Rokni, R.E. Klinkowstein, and S. Singer, "Expanding Beam Concept for Building Very Large Excimer Laser Amplifiers," Appl. Phys. Lett. 48, 318 (1986).
4. J.D. Jackson, "Classical Electrodynamics," Wiley, New York, pg. 139 (1962).
5. A.E. Siegman, "Unstable Optical Resonators for Laser Applications," Proc. IEEE, 53, 277, (1965).
6. D.W. Trainor, C. Londono-Hartmann, S. Fulghum, L. Litzenberger, et al., "XeF Laser Beam Quality Program, XeCl Long Pulse Laser Scaling Program," Technical Report CR-RD-DE-86-6, Avco Everett Research Laboratory Inc., March 1986.

Expanding beam concept for building very large excimer laser amplifiers

J. H. Jacob, M. Rokni,^{*} R. E. Klinkowstein
Science Research Laboratory Inc., Somerville, Massachusetts 02143

S. Singer
Los Alamos National Laboratory, Los Alamos, New Mexico 87545

(Received 7 August 1985; accepted for publication 7 October 1985)

Optical extraction efficiency from conventional lasers and amplifiers with nonsaturable intrinsic absorption is substantially below the maximum efficiency at absorption length products exceeding unity. This result is caused by the fact that high intensities in the amplifier cause saturation of gain but not absorption. In this letter, a new scalable amplifier concept is analyzed which maintains near maximum extraction efficiency as the laser length increases beyond absorption length products of unity.

In this letter a novel concept is presented for efficient volumetric scaling of excimer lasers to high average power and energy. This concept will enable one to efficiently scale excimer and exciplex lasers to energy and power levels a factor of 10 larger than that allowed by conventional geometry. Such a laser could, for example, be used for inertial confinement fusion. The active medium for a conventional geometry excimer laser is rectilinear in shape and is pumped by one or two high-energy electron beams which penetrate the high pressure laser mixture from two opposing faces of the laser cavity.¹ For active media with intrinsic nonsaturable absorption, the efficiency of a laser having this geometry decreases rapidly for absorption length products exceeding unity.^{1,2} For such absorption length products, the optical cavity flux increases along the length and the saturated gain decreases. The nonsaturable absorption, however, remains unchanged and so the efficiency of extracting photons from the active medium decreases.

The expanding beam concept discussed here removes this constraint by expanding the beam and maintaining near optimum cavity flux density during a single pass. Such an expansion can be accomplished by injecting a beam with spherical or cylindrical phase front into the amplifier. By solving the amplifier equation, we show that this concept can result in an efficiency improvement of a factor of 2 over the conventional rectilinear geometry in large scale amplifiers. Further, the angle at which the laser beam must be expanded is relatively small, 2°–5°. These small expansion angles are appropriate for using flow concepts developed for rectilinear amplifiers.

The amplification equation in a conventional rectilinear laser amplifier is given by

$$\frac{d\phi}{dx} = \frac{g_0\phi}{1+\phi} - \alpha_0\phi, \quad (1)$$

where g_0 is the small signal gain, α_0 the nonsaturable absorption coefficient, and $\phi = I/I_s$ is the intensity in units of the saturation flux. In writing Eq. (1) we have implicitly assumed that the steady state analysis is valid. This is true so long as the amplifier pulse length is much longer than the excimer lifetime. Typically the excimer lifetime is less than 10 ns

^{*}Permanent Address: The Racah Institute of Physics, The Hebrew University, Jerusalem, Israel

while the amplifier pulse length is of order 1 μ s, hence the steady state analysis is valid.

The extraction efficiency of an amplifier is given by

$$\eta_{ex} = (\phi_o - \phi_i)/\phi_{av}, \quad (2)$$

where ϕ_i and ϕ_o are the input and output fluxes respectively and ϕ_{av} is the maximum available flux which is given by

$$\phi_{av} = N^*h\nu L/(\tau I_s) = g_0L, \quad (3)$$

where N^* is the population inversion density, τ is the excited state lifetime, $h\nu$ is the laser photon energy, and L is the amplifier length. Solving Eq. (1) for given values of g_0 , α_0 , and ϕ_i , η_{ex} can be calculated as a function of amplifier length. Figure 1 shows plots of η_{ex} as a function of L for two values of ϕ_i , 0.1 and 1 and for the typical values of $g_0 = 2 \times 10^{-2} \text{ cm}^{-1}$ and $(g_0/\alpha_0) = 7$. The scaling of amplifier efficiency with length is apparent in the plots. For $\phi_i = 0.1$, the extraction efficiency first increases with increasing length and cavity flux, reaches a maximum of 30% at about 4.5 m, and then decreases with further increase of the length. For $\phi_i = 1$ the maximum extraction efficiency has a higher value (38%) which is reached at a length of 1.5 m. To understand this general behavior, a local extraction efficiency can be defined as²

$$\eta_{ex}(\text{local}) = \Delta\phi/\Delta\phi_{av}, \quad (4)$$

where $\Delta\phi_{av} = g_0\Delta x$ is the available flux along an incremental path length Δx . From Eqs. (1) and (4) it is easy to show² that there is an optimal flux given by $\phi_{opt} = (g_0/\alpha_0)^{1/2} - 1$ for which the local extraction efficiency is maximal with the value $\eta_{ex}(\text{local max}) = [1 - \alpha_0/g_0]^{1/2}$. In an amplifier with the conventional rectangular geometry the flux is in general smaller than the optimum flux at small lengths and larger than the optimum flux at large lengths. Therefore, the total extraction efficiency of the amplifier first increases with length, reaches a maximum, and then drops with further increase of the length.

To scale to large single pulse energy with an extraction efficiency close to the maximum, the local flux density must be maintained near its optimal value. This can be achieved by using the amplifier and the amplified beam in a matched expanding beam geometry as shown schematically in Fig. 2. In this case the beam expansion can be designed to compensate for the increase in flux density created by the gain of the

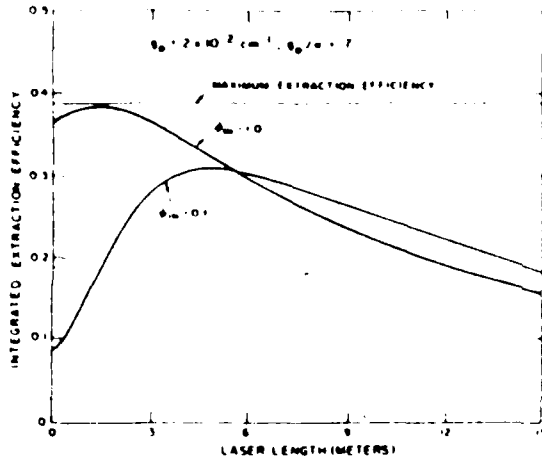


FIG. 1 Extraction efficiency as a function of length for a conventional rectangular amplifier with $g_0 = 2 \times 10^{-2} \text{ cm}^{-1}$ and $g_0/\alpha_n = 7$

active medium. The beam expansion can be two dimensional (spherical) or one dimensional (cylindrical) and the expansion angle can be selected to maximize the extraction efficiency for a desired length.

In an expanding beam amplifier $\phi = \phi[S(x), x]$, where $S(x)$ is the cross-sectional area and Eq. (1) is not applicable. Here the variation of ϕ is due to the variation of the cross-sectional area as well as gain and absorption and we have

$$\frac{d\phi}{dx} = \left(\frac{\partial\phi}{\partial S}\right) \frac{dS}{dx} + \left(\frac{\partial\phi}{\partial x}\right) \quad (5)$$

The second term in Eq. (5) is the variation of ϕ with x when S is constant and is given by Eq. (1). Substituting Eq. (1) into Eq. (5) one obtains

$$\frac{d\phi}{dx} = -\frac{\phi}{S} \frac{dS}{dx} + \frac{g_0\phi}{1+\phi} - \alpha_n\phi$$

Defining $\psi(x) = \phi(x)S(x)$ we get

$$\frac{d\psi}{dx} = S \frac{d\phi}{dx} + \phi \frac{dS}{dx} = \frac{g_0\psi}{1+\psi/S} - \alpha_n\psi \quad (6)$$

Comparing Eq. (6) with Eq. (1) we see that the beam expansion is equivalent to an increasing saturation flux with increasing length.

The extraction efficiency in this case is given by $\eta_{ext} = (\psi_o - \psi_i)/\psi_{av}$, where ψ_o and ψ_i are the output and input powers (in units of I_s) respectively and ψ_{av} is the available power given by

$$\psi_{av} = \frac{N^* h\nu V}{\tau I_s} = g_0 V, \quad (7)$$

where V is the volume of the amplifier

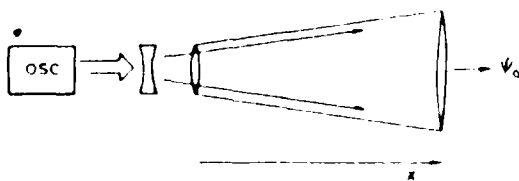


FIG. 2 Schematic geometry of an expanded beam amplifier

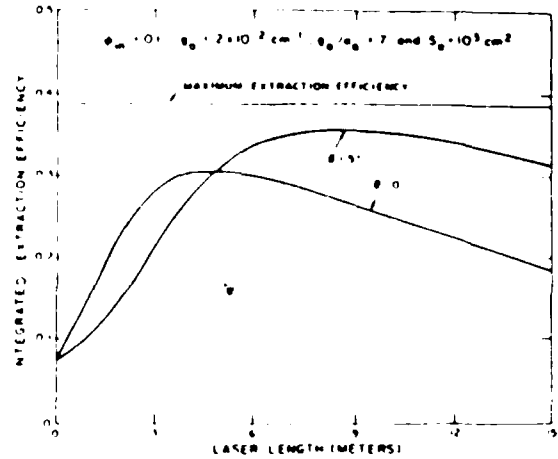


FIG. 3 Comparison between the length dependence of the extraction efficiency for an expanded beam amplifier and that for a rectangular amplifier, with $g_0 = 2 \times 10^{-2} \text{ cm}^{-1}$, $g_0/\alpha_n = 7$, and $\phi_m = 0.1$. The expanded beam amplifier is assumed to have a square cross section expanding in two dimensions with an angle of $\theta = 5^\circ$ and an entrance area of 10^3 cm^2

In Figs. 3 and 4 the dependence of the integrated extraction efficiency on amplifier length in an expanding beam amplifier is compared with that of a rectangular amplifier. The expanded beam amplifier is assumed to have a square cross section expanding in two dimensions at an angle $\theta = 5^\circ$ and an entrance area of $S_0 = 10^3 \text{ cm}^2$. The plots correspond to ϕ_m values of 0.1, small-signal gain of $g_0 = 2 \times 10^{-2} \text{ cm}^{-1}$, and $g_0/\alpha_n = 7$. From these figures the improvement in the integrated extraction efficiency at large lengths, obtained by using an expanding beam amplifier concept, is obvious. For the largest length of 15 m, the expanding beam amplifier has an extraction efficiency of twice the conventional rectangular amplifier

From these results we can conclude that for a gain medium with nonsaturable intrinsic absorption, the expanding beam geometry allows laser amplifiers to be scaled to large

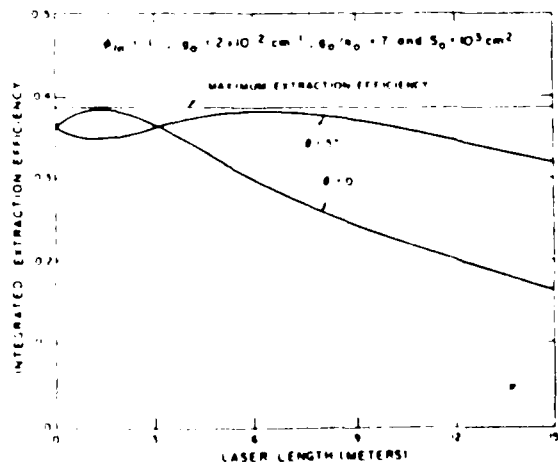


FIG. 4 Comparison between the length dependence of the extraction efficiency for an expanded beam amplifier and that for a rectangular amplifier $\phi_m = 1$ and the rest of the parameters as in Fig. 3

lengths while maintaining integrated extraction efficiencies close to the maximum value. An additional advantage of the expanding wave amplifier is the reduced adverse effects resulting from amplified spontaneous emission. This is because the gain is more uniformly saturated in the expanded

beam geometry than in the conventional rectilinear amplifiers.

¹See, for example, M. Rokni, J. A. Mangano, J. H. Jacob, and J. C. Hsia, *IEEE J. Quantum Electron.* QE-14, 464 (1978).

²W. W. Rigrod, *IEEE J. Quantum Electron.* QE-14, 377 (1978).

END

8-87

DTIC